Superconducting wigglers and undulators

Mezentsev Nikolay

**Budker institute of Nuclear Physics,
Novosibirsk, Russia**

Content

Introduction

3-pole wiggler (shifter) –main objective is an increasing of radiation rigidity. The central pole is used as a radiation source. The point of radiation is shifted of relatively initial orbit. All three bending magnets are superconducting.

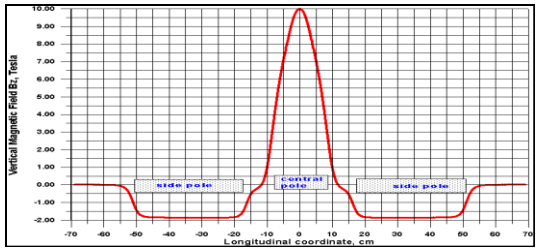

Shifter with the fixed radiation point – The same objective as previous one. The central pole is used as a radiation source. The external normally conducting magnets are used to keep beam orbit on a straight section axis at change of the main field.

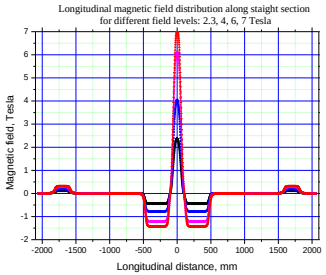

Superconducting multipole wiggler – main objective - generation of powerful synchrotron radiation with high photon flux density in the rigid X-ray range. (K>>1)

$$K = 0.934 \cdot \lambda_0[\mathrm{cm}] B_0[\mathrm{T}]$$

K~1 - undulator.
K>>1 - wiggler

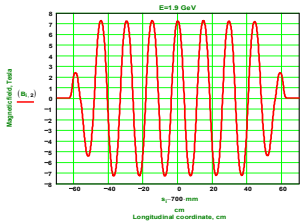

Superconducting undulator – a basic purpose – generation of spatially coherent undulator radiation of high. (K ~ 1)

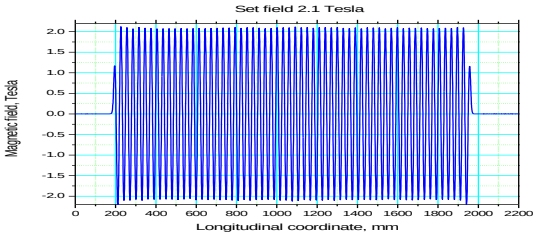

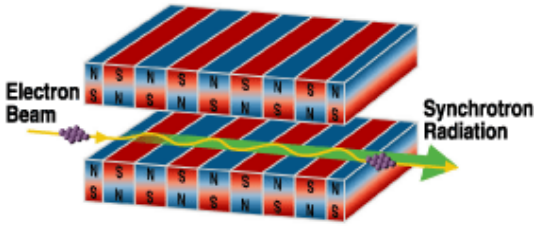

History

First superconducting multipole wiggler, BINP, Russia - 1979

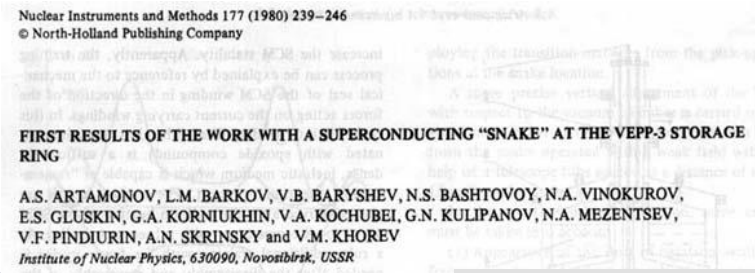
Nuclear Instruments and Methods 177 (1980) 239–246
© North-Holland Publishing Company

FIRST RESULTS OF THE WORK WITH A SUPERCONDUCTING "SNAKE" AT THE VEPP-3 STORAGE RING

A.S. ARTAMONOV, L.M. BARKOV, V.B. BARYSHEV, N.S. BASHTOVOY, N.A. VINOKUROV, E.S. GLUSKIN, G.A. KORNIUKHIN, V.A. KOCHUBEI, G.N. KULIPANOV, N.A. MEZENTSEV, V.F. PINDIURIN, A.N. SKRINSKY and V.M. KHOREV

Institute of Nuclear Physics, 630090, Novosibirsk, USSR

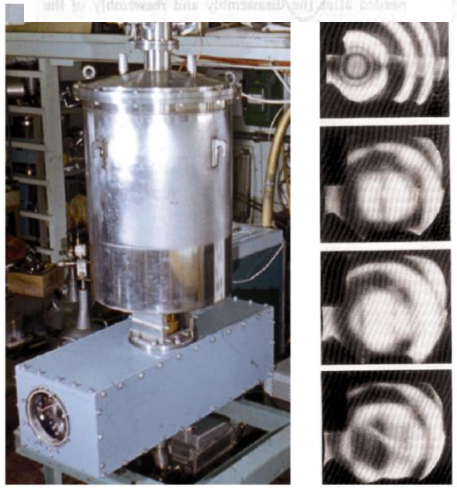

(A) (B)

A) The wiggler cryostat with magnet
B)Undulator radiation from the wiggler through red filter

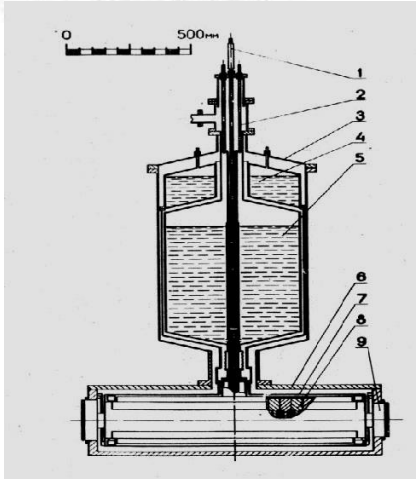

Sketch of the wiggler cryostat

Pole number	20
Pole gap, mm	15
Period, mm	90
Magnetic field amplitude, T	3.5
Vertical beam aperture, mm	7.8

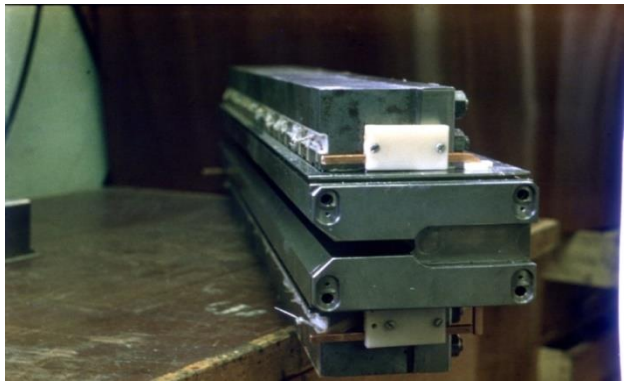

Photo of the wiggler magnet

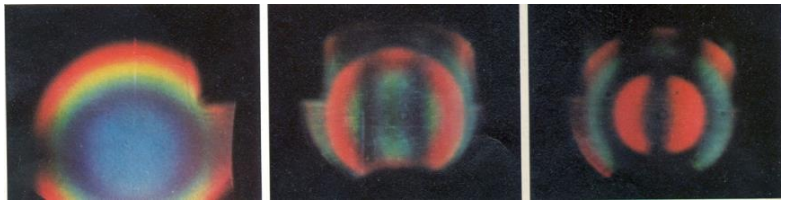

E=350 MeV

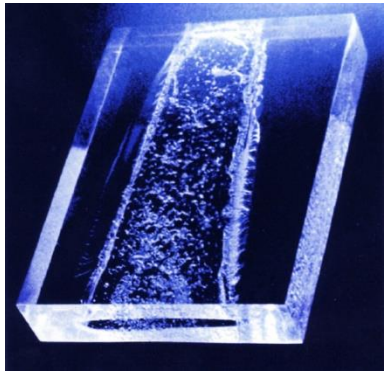

Ablation of PMMA (organic glass) due to treatment of SR beam from superconductive wiggler Installed on VEPP-3 storage ring (Novosibirsk, 1979) E=2 GeV, B~3 Tesla

History

First superconducting helical undulator, Stanford University - 1973

L. Elias and J. Madey, "Superconducting helically wound magnet for the free electron laser," Review of Scientific Instruments, vol. 50, no. 11, pp. 1335-1340, 1979.

The very first SCU has been designed and built by J.Madey's group at Stanford University in 1973. This 5-m long helical SCU with the period of 32.3 mm used for pioneering FEL experiment . The choice of the superconducting technology was driven by necessity to achieve the maximum undulator K value. And since permanent magnets at that time have not been yet introduced as a material of choice for building undulators, the logical, although quite challenging step was to enhance electromagnet technology with superconducting conductor to achieve higher magnetic field. The attempt was a success, and J.Madey and his colleagues for the first time successfully demonstrated the viability of high gain FEL. (Efim Gluskin)

History

First superconducting planar undulator, ACO, Orsay, France -1980

Tome 41 N° 23 1er DÉCEMBRE 1980

LE JOURNAL DE PHYSIQUE - LETTRES

J. Physique — LETTRES **41** (1980) L-547 - L-550 1er DÉCEMBRE **1980**, PAGE L-547

Classification
Physics Abstracts
41.70 — 42.72

First results of a superconducting undulator on the ACO storage ring (*) (**)

C. Bazin ([1]), M. Billardon ([2]), D. Deacon ([3]) ([†]), Y. Farge, J. M. Ortega ([2]), J. Pérot ([4]), Y. Petroff and M. Velghe ([5])

LURE, Bât. 209 C, Université de Paris-Sud, 91405 Orsay, France.

Abstract. A superconducting undulator has been fixed on the ACO storage ring. It has been observed that the electron beam is stable in the small gap of the vacuum chamber and unperturbed by the magnetic field of the undulator. Light emission has been observed at 140 and 240 MeV in the visible and ultra-violet. First results indicate that its geometrical as well as spectral distribution agree with theoretical predictions; small disagreements
very probably arise from the fact that the electrons are not travelling exactly on the axis of the undulator.

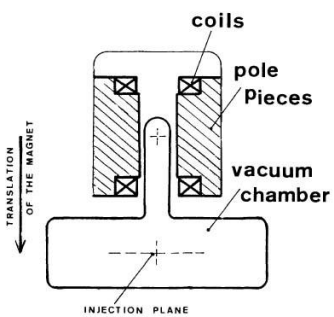

Period	40 mm
Number of periods	23
Effective length	0.96 m
Maximum field Bo	0.45 T (K = 1.68).

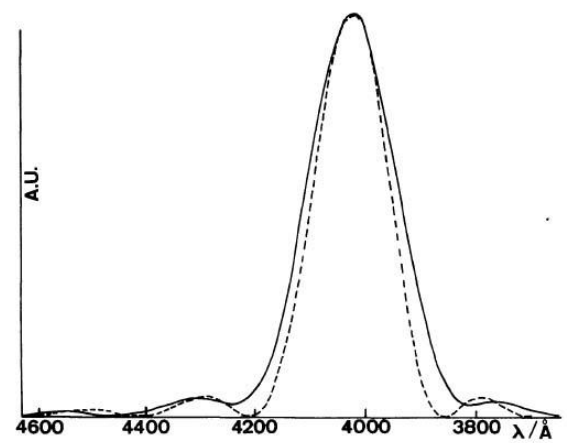

Fig. 4. — Spectral distribution of the emitted light (E = 150 MeV, K = 1.2) through a very small pinhole in the horizontal plane. Experiment : full lines ; Theory : dashed lines.

Superconductors

B-T (critical field-critical temperature) and B-J (critical field – critical current) diagrams are shown in the figures below for best low temperature superconductors. Most of them exceed superconductors NbTi and Nb_3Sn by maximal magnetic field. However they, as a rule, essentially are more complex in manufacturing, and only two materials V_3Ga and Nb_3Al are possible to receive in the comprehensible form and the sufficient length for winding.

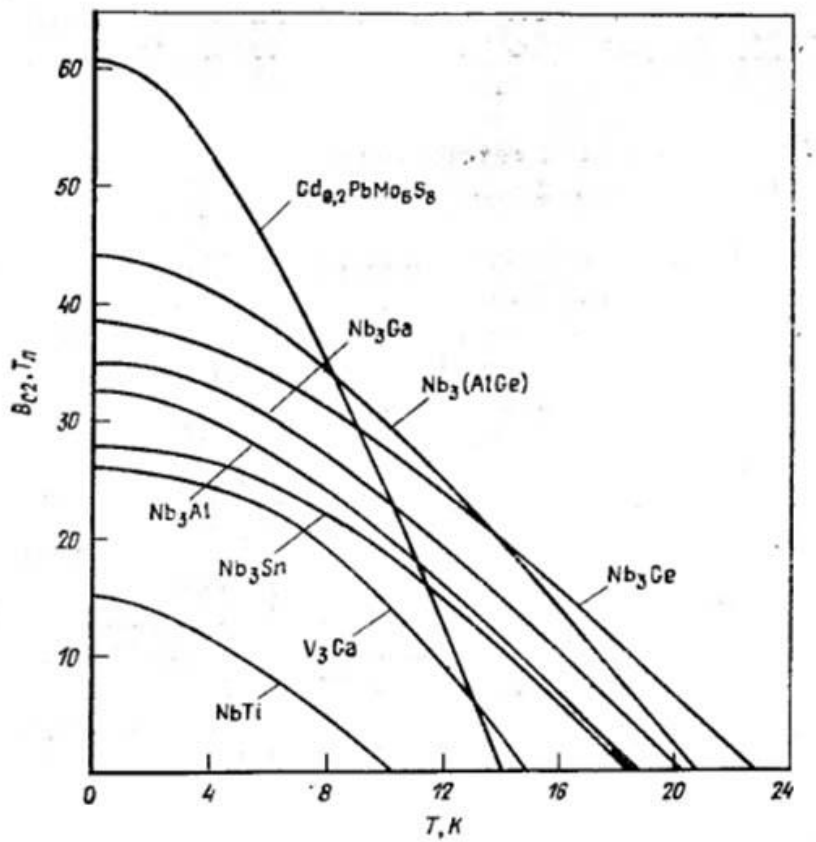

B-T critical curves of most popular SC materials for current in superconductors J=0A

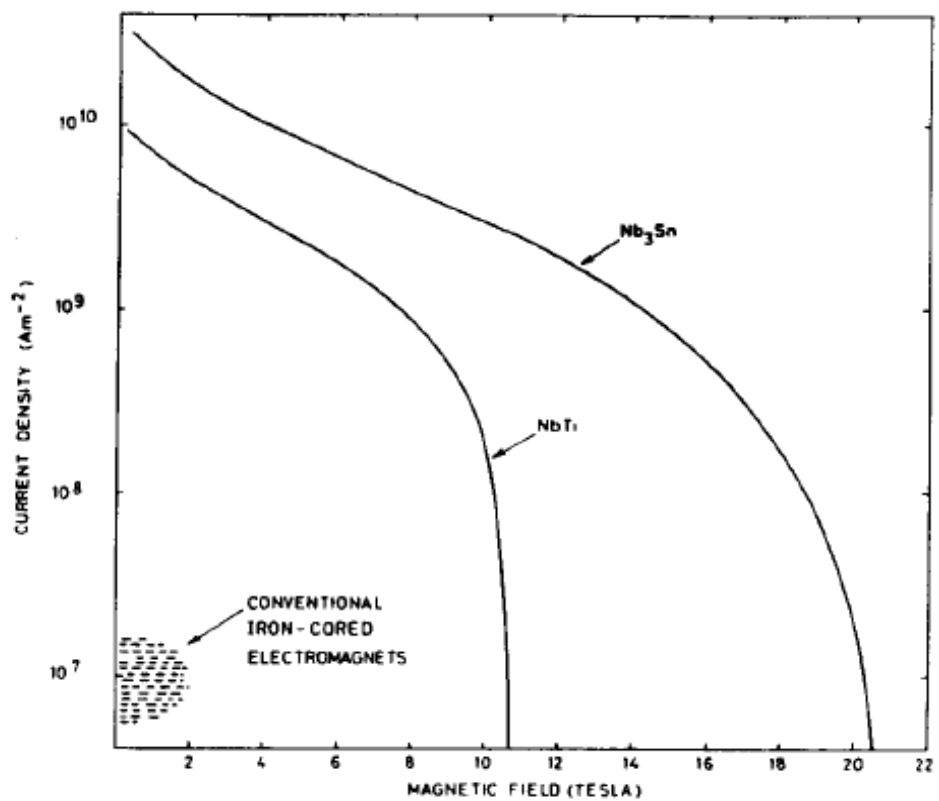

B-J diagrame of Nb_3Sn and NbTi superconductors for 4.2K temperature

Nb-Ti/Cu SC wire

NbTi/Cu superconductor began one of the first to be used as a material suitable for magnet manufacturing. Owing to reliability and simplicity of windings manufacturing it still is the basic superconducting material for various magnets with field up to 8T.

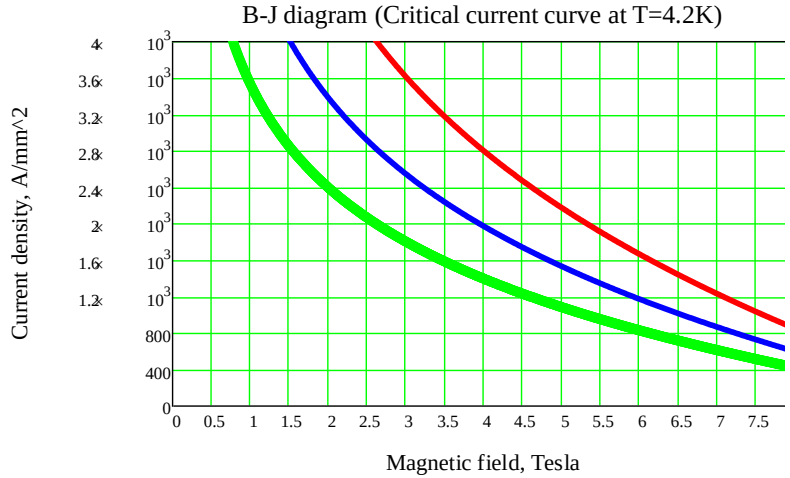

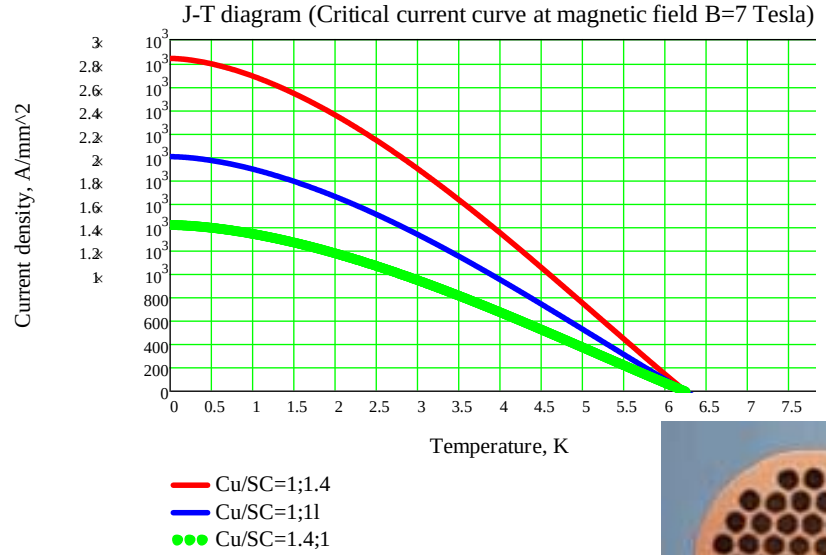

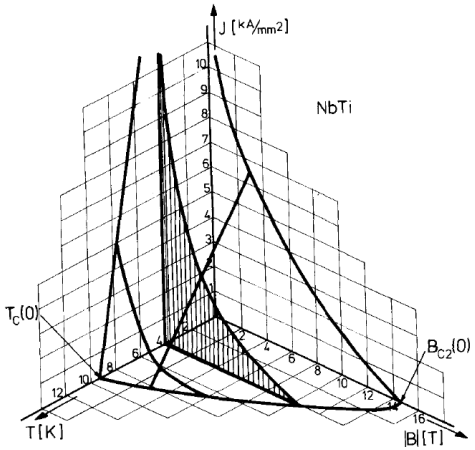

NbTi/Cu wire cross section

Bottura's formula

B_{C2} ~ 14.5 Tesla at T=0K, T_{C0} ~9.2K at B=0T.

$$B_{C2}(T) = B_{C20}\left[1-\left(\frac{T}{T_{C0}}\right)^{1.7}\right]$$

$$\frac{J_C(B,T)}{J_{Cref}} = \frac{C_0}{B}\left[\frac{B}{B_{C2}(T)}\right]^{\alpha}\left[1-\frac{B}{B_{C2}(T)}\right]^{\beta}\left[1-\left(\frac{T}{T_{C0}}\right)^{1.7}\right]^{\gamma}$$

C_0, α, β и γ – empirical parameters

Typical values: C_0=30T, α=0.6, β=1 и γ=2

Superconductors

Nb_3Sn/Cu SC wire

Magnet manufacturing with use of superconductors on base of Nb3Sn/Cu demands much more complex technology connected with baking out of a ready magnet at high temperature in vacuum or inert gas.

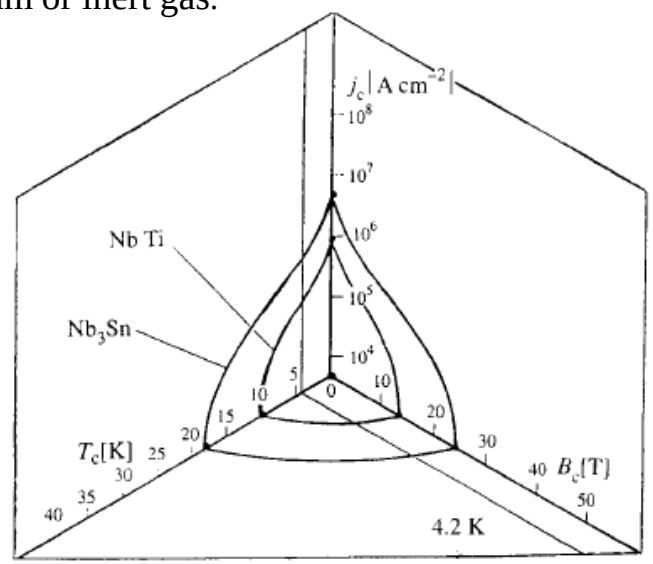

$$\frac{B_{C2}(T,\varepsilon)}{B_{C20}(\varepsilon)} = \left[1-\left(\frac{T}{T_{C0}(\varepsilon)}\right)^2\right]\cdot\left\{1-0.31\cdot\left(\frac{T}{T_{C0}(\varepsilon)}\right)^2\cdot\left[1-1.77\ln\left(\frac{T}{T_{C0}(\varepsilon)}\right)\right]\right\}$$

$B_{C20} = 30T$ critical field at T=0K

$T_{C0} = 18K$ critical temperature at B=0T

ε – deformation $T_{C0}(\varepsilon) = T_{C0m}\cdot\left(1-a\cdot|\varepsilon|^{1.7}\right)^{\frac{1}{3}}$

a =900 for compressive deformation

a=1250 for tensile deformation

Four main processes of fabricating Nb_3Sn wires:

- Bronze process
- Internal Sn process
- Powder in tube (PIT) process
- RRP (Restacked Rod Process)

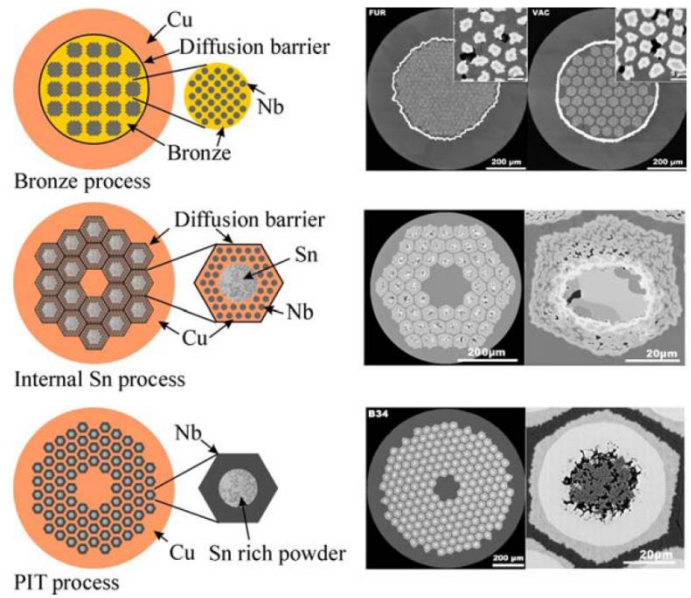

RRP process

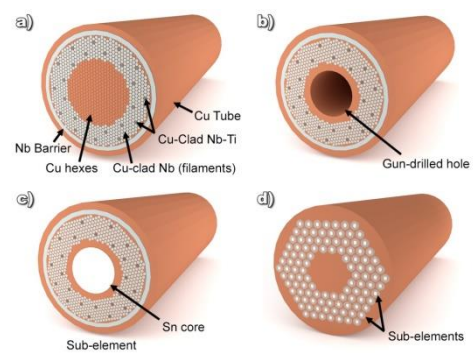

Influence of SC ID field on beam dynamics

Orbit inside ID

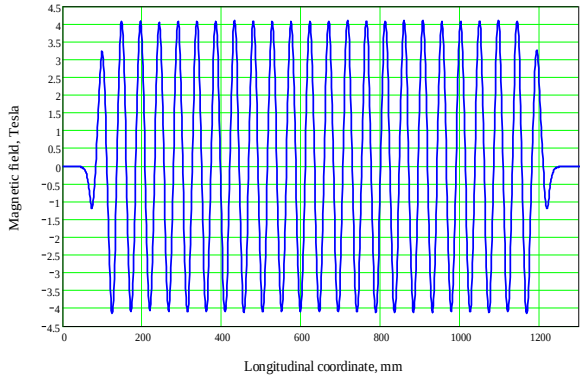

$$B_z = B_0 \cos(k_0 s)\cos(k_x x)\cosh(k_z z)$$

$$B_x = -\frac{k_x}{k_z} B_0 \cos(k_0 s)\sin(k_x x)\sinh(k_z z)$$

$$B_s = -\frac{k_0}{k_z} B_0 \sin(k_0 s)\cos(k_x x)\sinh(k_z z)$$

$$k_z^2 = k_0^2 + k_x^2$$

k_0, k_x, k_z - wiggler wave numbers

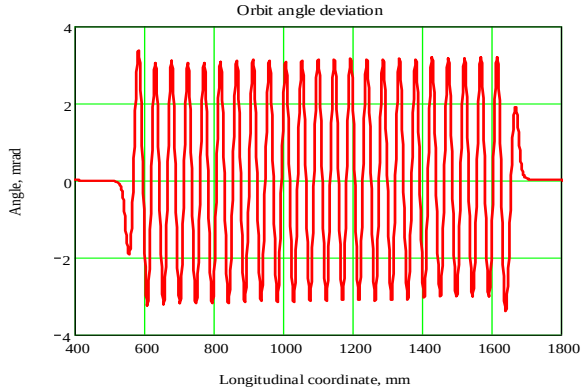

$$I_1^x(s) = \int_{-L/2}^{s} ds' B_z(s'),$$

First field integral

$$x_0'(s) = \frac{I_1^x(s)}{B\rho}$$

Angle of electron orbit
Inside a wiggler

Angle orbit deviation inside 49-pole wiggler at field setting 4.2 Tesla, E=3 GeV

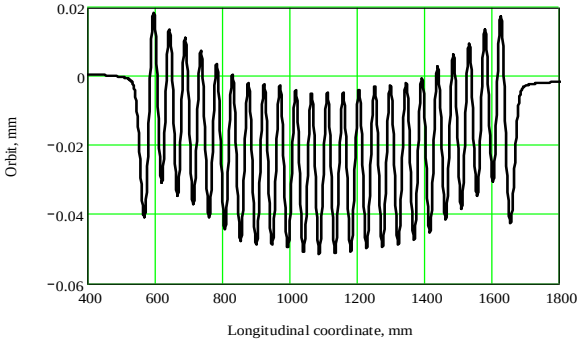

$$I_2^x(s) = \int_{-L/2}^{s} ds' \int_{-L/2}^{s'} ds'' B_z(s'')$$

Second field integral

$$x_0(s) = \frac{I_2^x(s)}{B\rho}$$

Electron orbit
Inside a wiggler

Orbit distortion inside 49-pole wiggler at field setting 4.2 Tesla, E=3 GeV

Phase spaces of electron orbit and photon beam

Electron beam orbit phase space

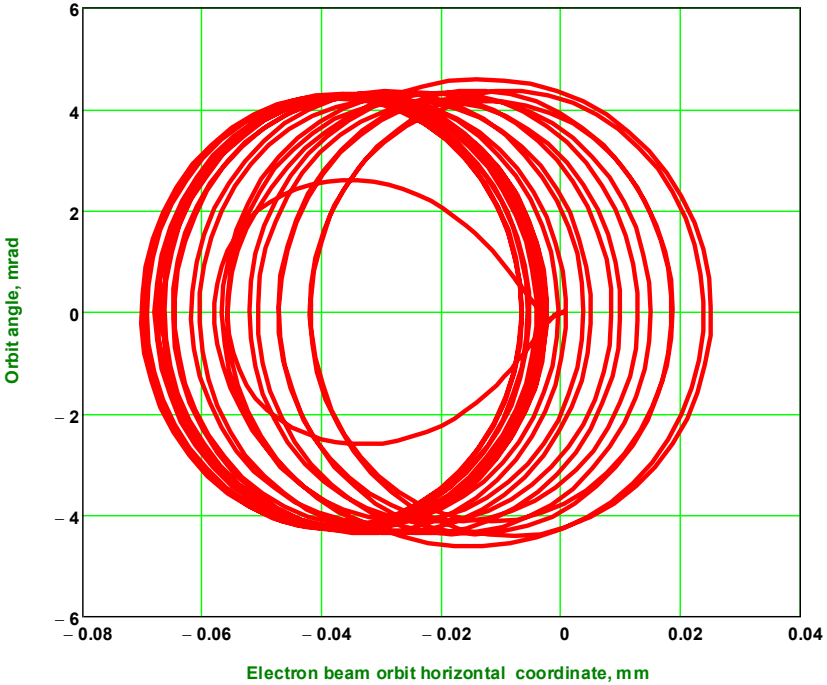

Photon beam phase space reduced to the wiggler center

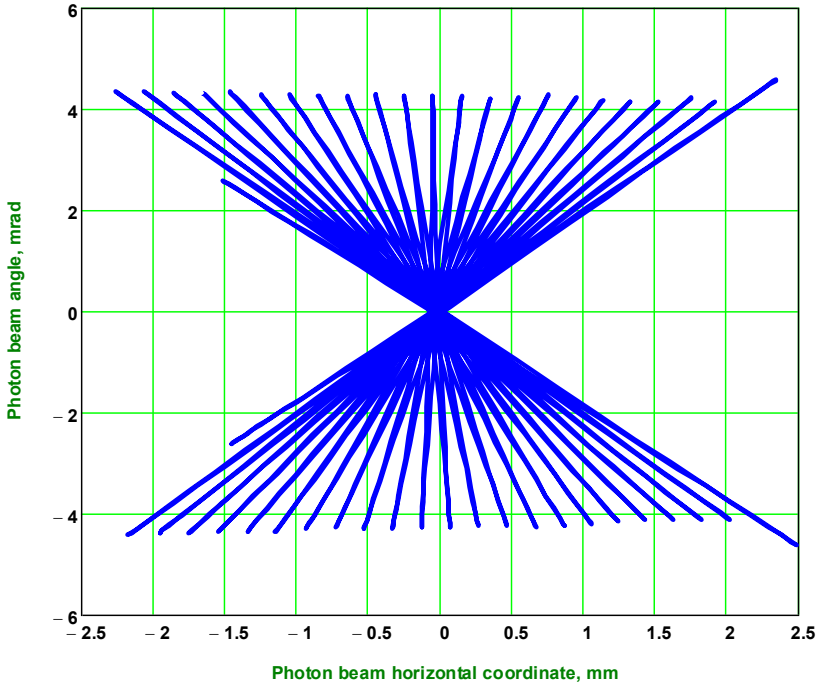

Beam focusing

The wiggler can be a strong focusing element in a magnetic structure of a storage ring and create betatron tune shifts and perturbations of Twiss functions. In the ideal case of a symmetric magnetic structure of a multipole wiggler there is only a B_z field component in the median plane-plane of symmetry. Any deviation from that plane introduces longitudinal field B_y that could be found from the expression:

$$B_y = \frac{dB_z}{dy} \cdot z \qquad B_x = \frac{dB_z}{dy} \cdot z \cdot \frac{dx_0}{dy}$$

In accompanying electron beam orbit x_0 coordinate system rotated by orbit angle $\frac{dx_0}{dy}$ relative to the coordinate system of the wiggler, the field component B_y has a projection on the x-axis.

$$\frac{d^2x}{dy^2} + K_x \cdot x = 0 \qquad \frac{d^2z}{dy^2} + K_z \cdot z = 0$$

$$K_x = \frac{B_z^2}{B\rho^2} + \frac{1}{B\rho}\left(\frac{dx_0}{dy} \cdot \frac{\partial B_z}{\partial y} - \frac{\partial B_z}{\partial x}\right); \quad K_z = -\frac{1}{B\rho}\left(\frac{dx_0}{dy} \cdot \frac{\partial B_z}{\partial y} - \frac{\partial B_z}{\partial x}\right)$$

Effective focusing functions

The integral values of K_x and K_z at the length L of the wiggler magnet will be equal:

$$\int K_z\, dy = \frac{B_0^2}{2B\rho^2}\left(1 + \frac{k_x^2}{k_0^2}\right)L \qquad \int K_x\, dy = \frac{-B_0^2}{2B\rho^2}\left(\frac{k_x^2}{k_0^2}\right)L$$

Beam focusing and multipole components

$$\Delta\nu_{x,z} \approx \frac{K_{x,z} L \beta_{x,z}}{4\pi}\left(1 + \frac{L^2}{12\beta_{x,z}^2}\right)$$

If magnetic system is homogeneous enough so that orbit deviation is much less than characteristic size of field decrease, the formulas may be simplified:

δ – a shift off wiggler axis in x direction,
Lw – wiggler length,
Bρ- beam rigidity

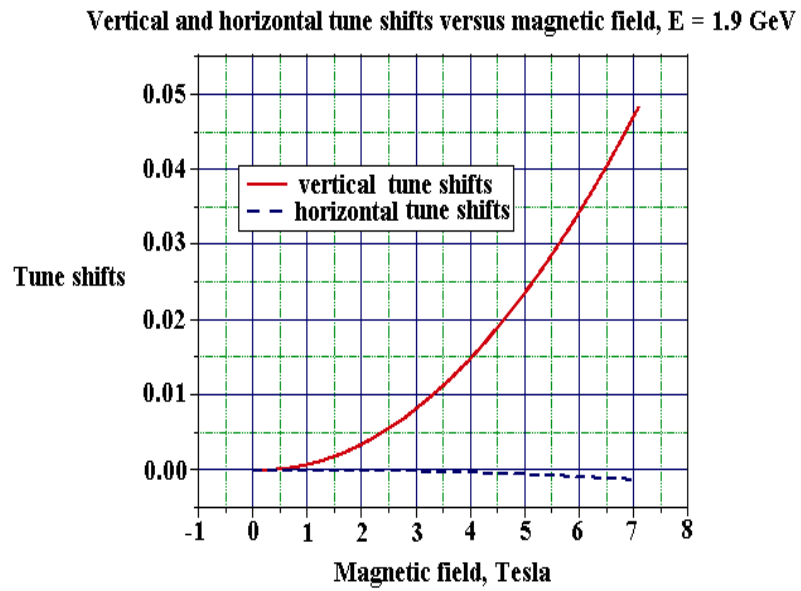

Vertical and horizontal betatron tune shifts for BESSY SC 7 T WLS versus magnetic field level.

First field integral

$$\int B_z(s)ds = \frac{B_0^2}{2B\rho}\frac{k_x^2}{k_0^2}L_w\delta$$

Gradient integral in vertical direction

$$\int G_v(s)ds = \frac{B_0^2}{2B\rho}\left(1 + \frac{k_x^2}{k_0^2}\right)L_w$$

Gradient integral in horizontal direction

$$\int G_h(s)ds = -\frac{B_0^2}{2B\rho}\frac{k_x^2}{k_0^2}L_w$$

Sextupole integral

$$\int S(s)ds = \frac{B_0^2}{2B\rho}\left(2 + \frac{k_x^2}{k_0^2}\right)k_x^2 \cdot \delta \cdot L_w$$

Octupole integral

$$\int O(s)ds = -\frac{3B_0^2}{8B\rho}\left(4k_x^2 + \frac{B_0^2}{B\rho^2}\right)L_w$$

Radiation (structural) integrals:

$$\Delta I_1 = \int_L \frac{(\eta_{x0} - x(s))B_z(s)}{B\rho} ds$$

$\alpha_x, \beta_x, \gamma_x$ are Twiss parameters

$$\Delta I_2 = \int_L \frac{B_z^2(s)}{B\rho^2} ds$$

$$\Delta I_3 = \int_L \frac{|B_z(s)|^3}{B\rho^3} ds$$

$$\Delta I_4 = \int_L \left(\frac{B_z^3(s)\cdot}{B\rho^3} - \frac{2K_x}{B\rho} \right) (\eta_{x0} - x(s)) ds$$

$$\Delta I_5 = \int_L \frac{|B_z(s)|^3}{B\rho^3} \left(\gamma_x (\eta_{x0} - x(s))^2 + 2\alpha_x (\eta_{x0} - x(s))(\eta'_{x0} - x'(s)) + \beta_x (\eta'_{x0} - x'(s))^2 \right) ds$$

$$\left(\frac{\sigma'_E}{\sigma_E} \right)^2 = \frac{1 + \frac{\Delta I_3}{I_3^0}}{1 + \frac{2\Delta I_2 + \Delta I_4}{2I_2^0 + I_4^0}} \approx 1 + \frac{\Delta I_3}{I_3^0} - \frac{\Delta I_{24}}{I_2^0}$$

Energy spread change

$$\frac{\varepsilon'_x}{\varepsilon_x} = \frac{1 + \frac{\Delta I_5}{I_5^0}}{1 + \frac{\Delta I_2 - \Delta I_4}{I_2^0 - I_4^0}} \approx 1 + \frac{\Delta I_5}{I_5^0} - \frac{\Delta I_2}{I_2^0}$$

Emittance change

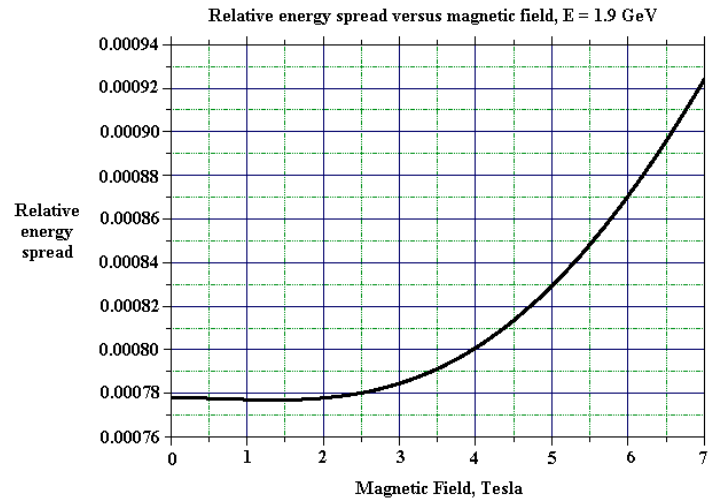

Energy spread in BESSY storage ring versus magnetic field level in SC 7 T WLS.

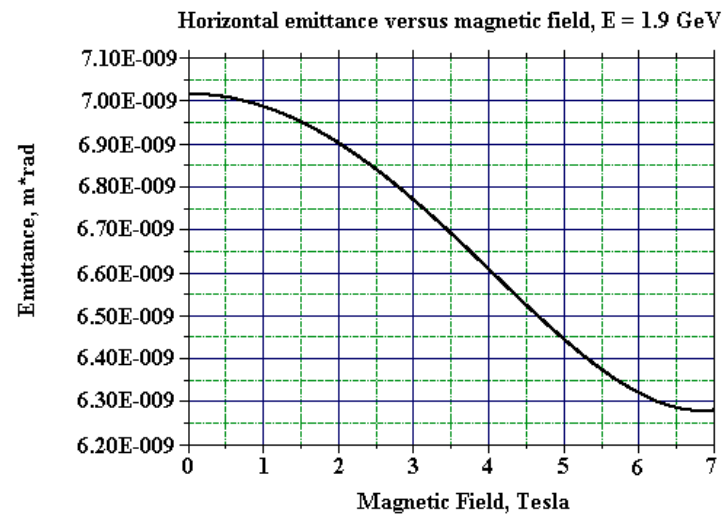

Horizontal emittance BESSY storage ring versus magnetic field level in SC 7 T WLS.

SC coils design of multipole wigglers and undulators

Superconducting coils:

•Horizontal racetrack coils

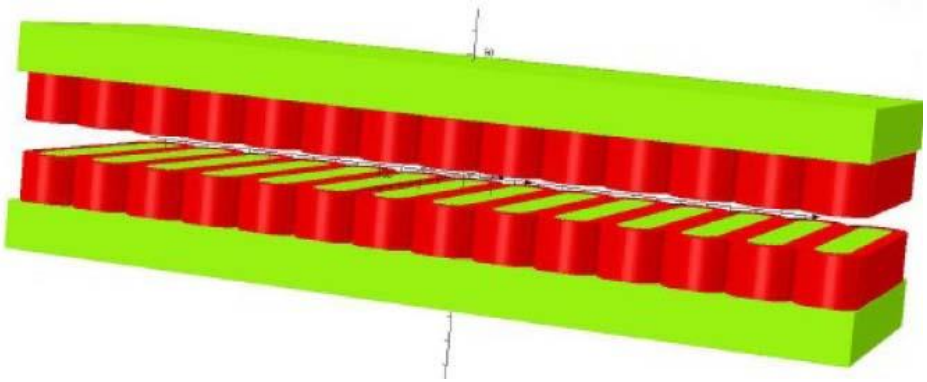

•Vertical racetrack coils

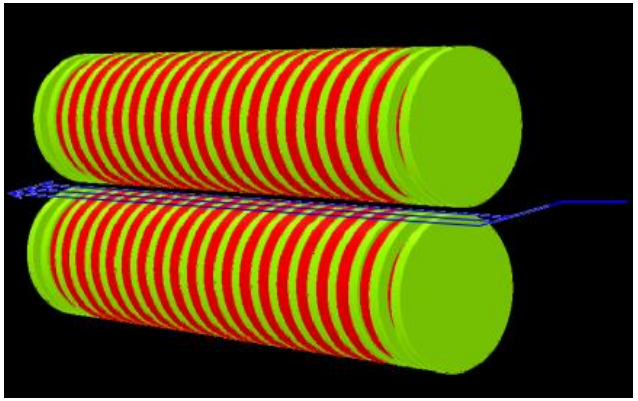

Horizontal racetrack	Vertical racetrack
Short SC wire is required	Long SC wire is required
Large number of splices for large number of poles.	Less number of splices.
Total SC wire length is minimal	Total SC wire length is 3-4 time more.
There is a possibility to make multi sections coils	There is no possibility to make multi section coils
The coils are stressed by bronze rods to compensate magnetic pressure in coils.	There is no possibility to stress coils by external compression
Minimal stored magnetic energy and inductance	Stored energy and inductance is more by 3 times
The coils have good thermo contacts with iron yoke after cooling down due to external compression	The thermo contacts became worth after cooling down. This is important disadvantage for indirect cooling magnets

Superconducting coils:

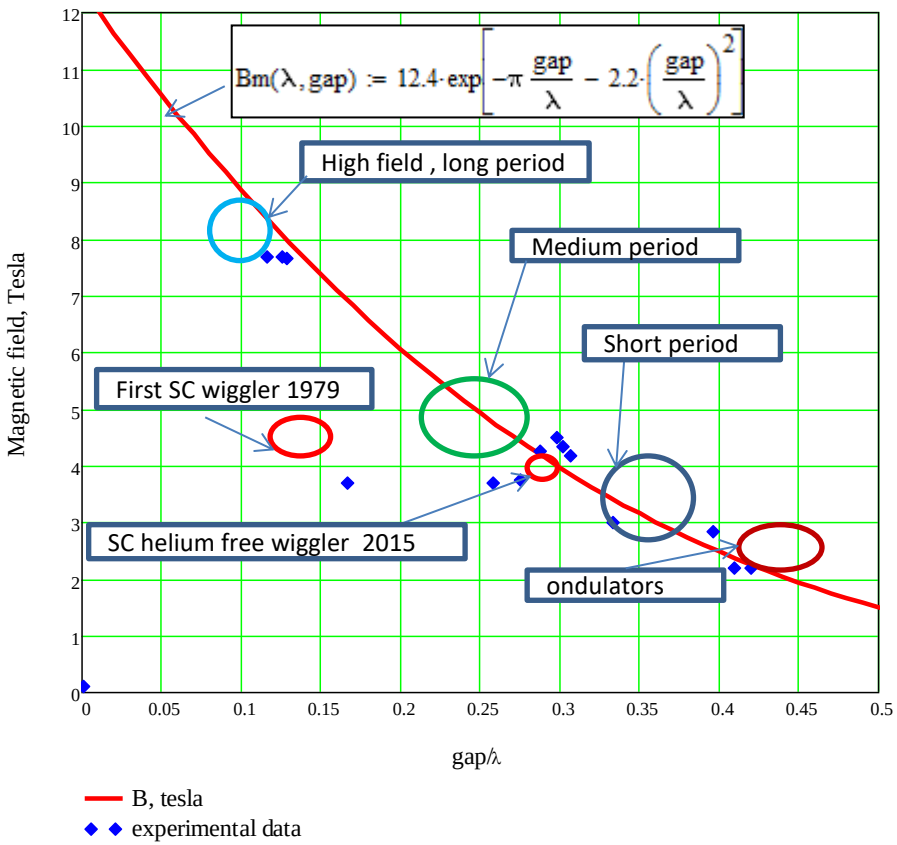

Depending on parameter K the multipole superconducting insertion devices, based on NbTi/Cu wire, may be devided into 4 groups of popularity of use.

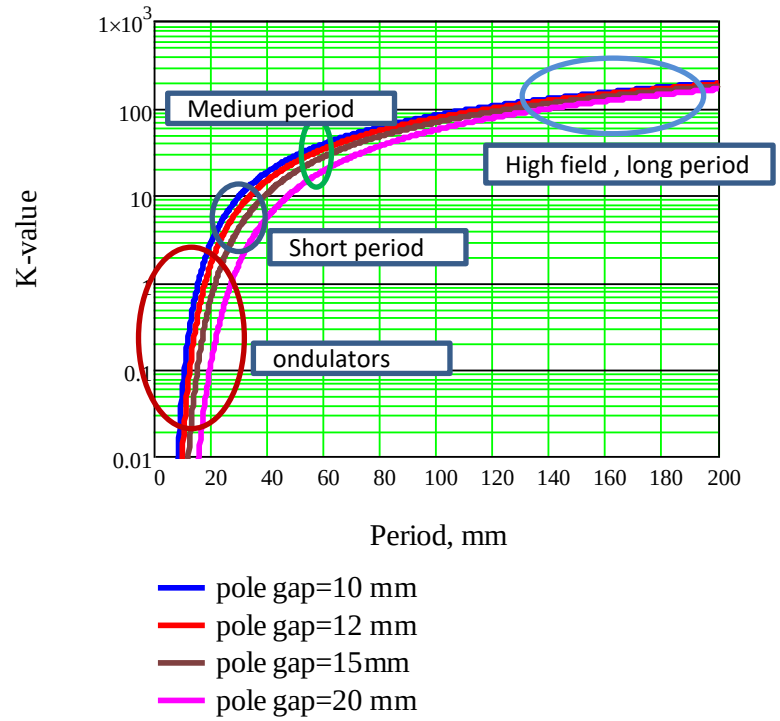

The dependence of the peak magnetic field in the median plane on the ratio g/λ for superconducting wigglers, made using low-temperature superconductor NbTi/Cu. The blue points correspond to the real wigglers with different periods and pole gaps. The red curve corresponds to the formula for the peak field evaluation.

2-sections coils (example, SC wiggler)

Period, mm	48
Pole gap, mm	14.4
Pole number	49
Nominal field, T	4.1

Wire parameters:

Wire diameter with/without insulation, mm	**0.91/0.85**
NbTi/Cu ration	**1.4**
Number of filaments	**312**
Diameter of filament, micron	**37**
Critical current at 7 Tesla, A	**700**

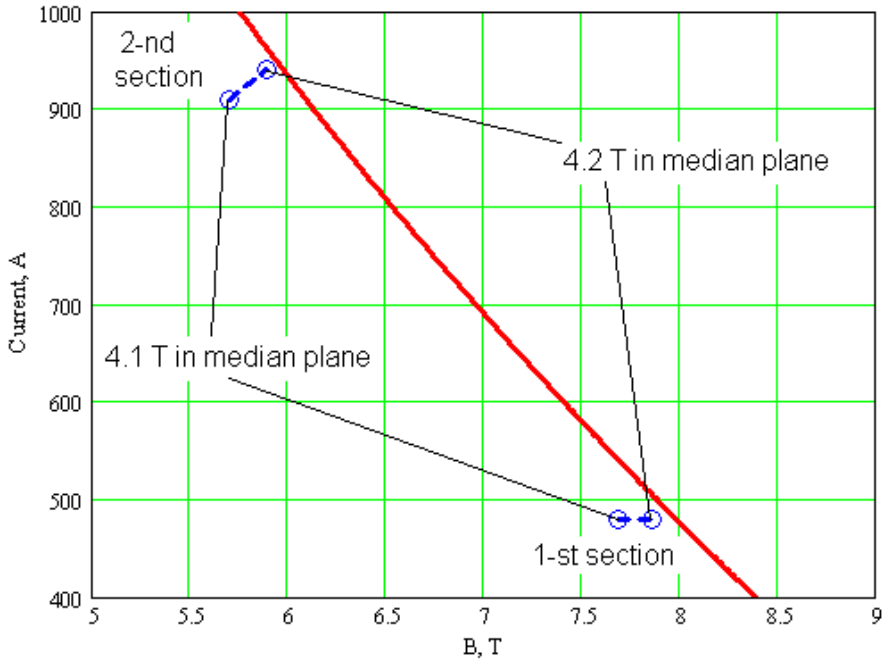

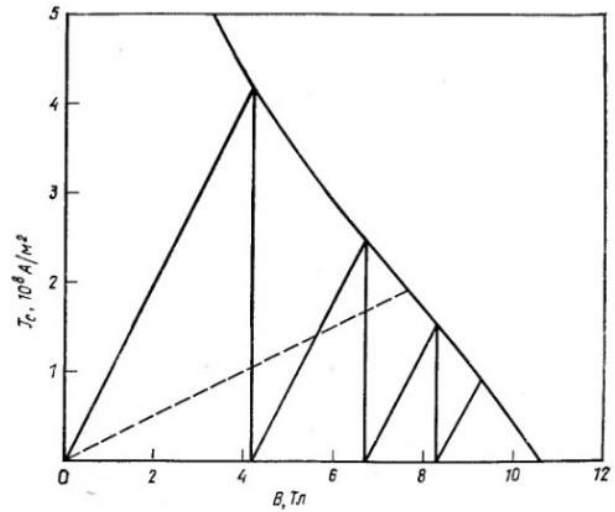

Load lines for 4-section magnet with separate feeding

Critical current curve of used superconducting Nb-Ti wire (red line) and field-current critical points inside coil correspond to magnetic field in median plane

Two-sections coil gives up to 15% higher field for the same SC wire.

Magnetic field distribution in high field wigglers (Example of 7.5 T SC wiggler)

The magnetic flux inside of a pole in multipole wigglers and undulators is closing through the neighbor poles. In case of 2-dimensional field distribution (infinitely wide poles) the longitudinal field integral in median plane is automatically equal to zero. It follows from Maxwell's equations. At a high field in a wiggler iron cores are completely saturated and represent permanent magnets which give to the field some small contribution. The maximal field inside the coils is on a wire layer which is nearest to an iron pole and approximately on half of height of the pole. This fact should be taken into account at field calculation as this part of the wire is most close to a critical curve on the diagram a field-current. External iron yoke is in use mainly as support system for poles and closes a stray field.

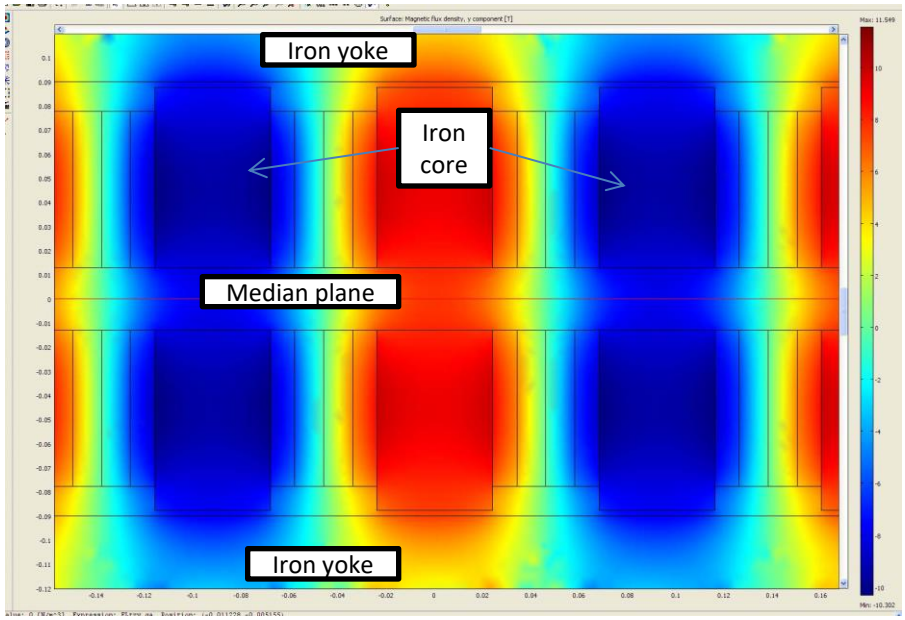

Vertical component of magnetic field distribution

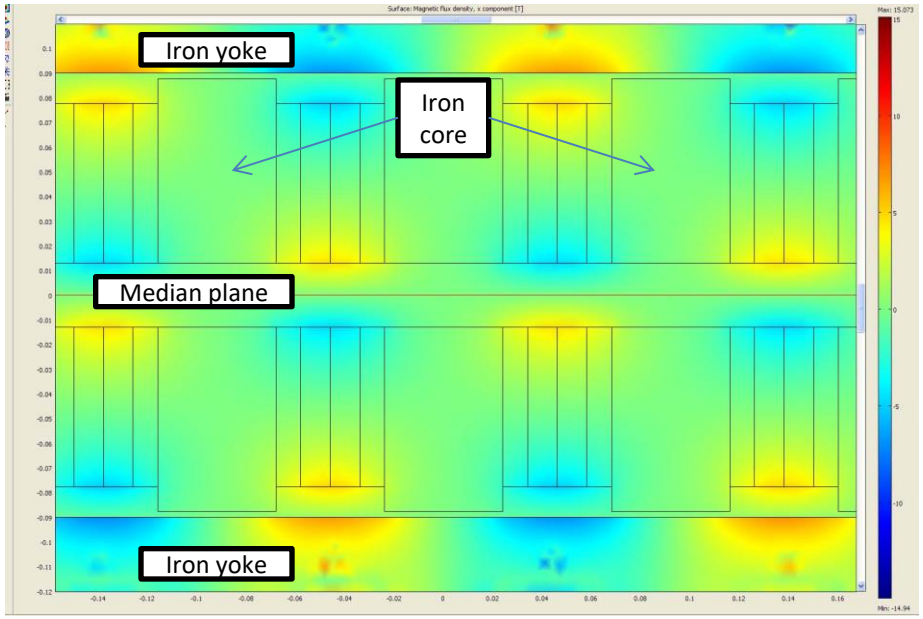

Horizontal component of magnetic field distribution

Ampère forces in high field SC wigglers (Example of 7.5 T SC wiggler)

The forces acting on windings in horizontal direction, aspire to tear off the winding from the iron core. If there is no counteracting force a winding may move and as a result a heat will be extracted, temperature of a superconducting wire will rise up and the wire may transit to normal state (quench). Usually in such situations the further quench training of the magnet does not lead to field increasing. Presence of counteracting force may create a high pressure inside of windings (several hundreds bar) at which epoxy starts to crack with heat extraction. This also may be a reason of a quench. But here there is a hope, that quench training increase the field.

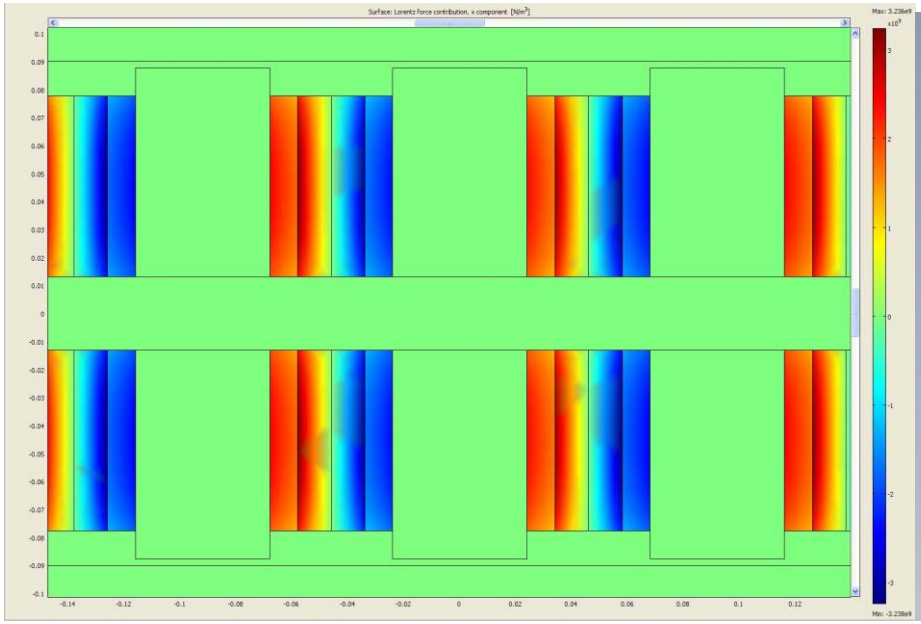

Distribution of horizontal component of Ampère forces acting on windings

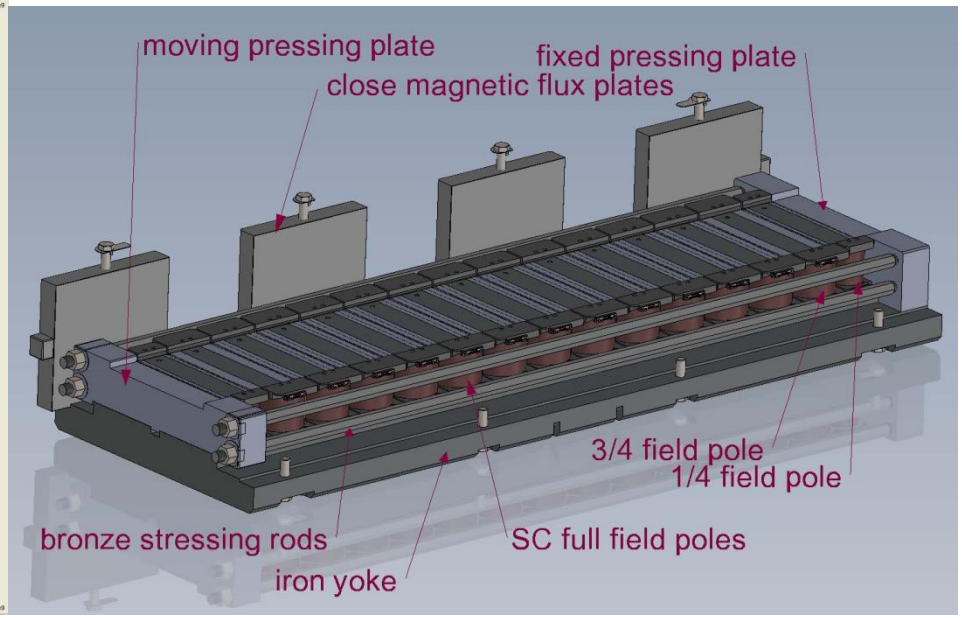

Drawing of half of a high field superconducting wiggler

Ampère forces in high field SC wigglers (Example of 7.5 T SC wiggler)

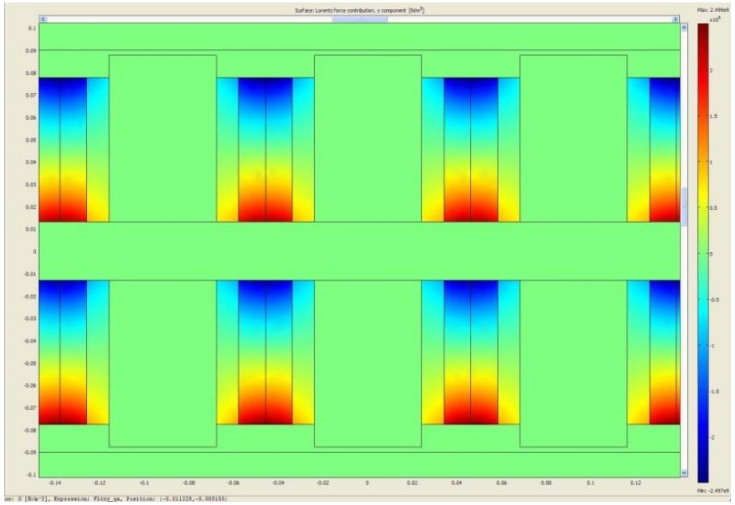

Ampère forces (vertical component) acting on windings in vertical direction

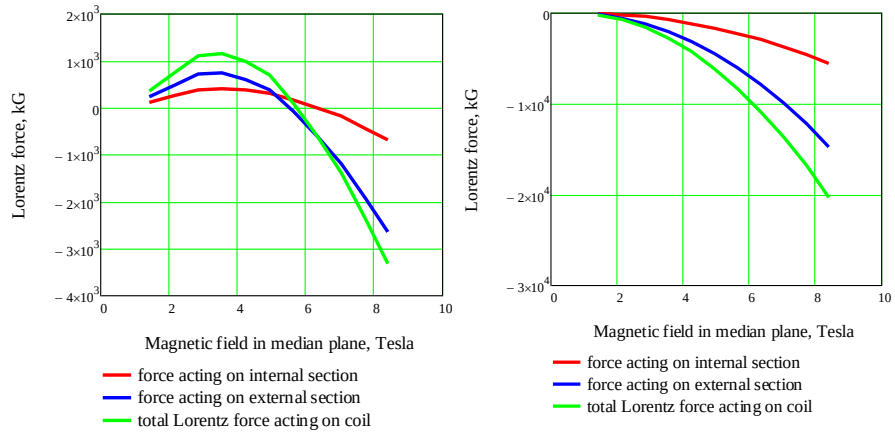

A B

Integral forces acting on coil sections versus field level . A) wiggler with iron yoke. B) wiggler without iron yoke.

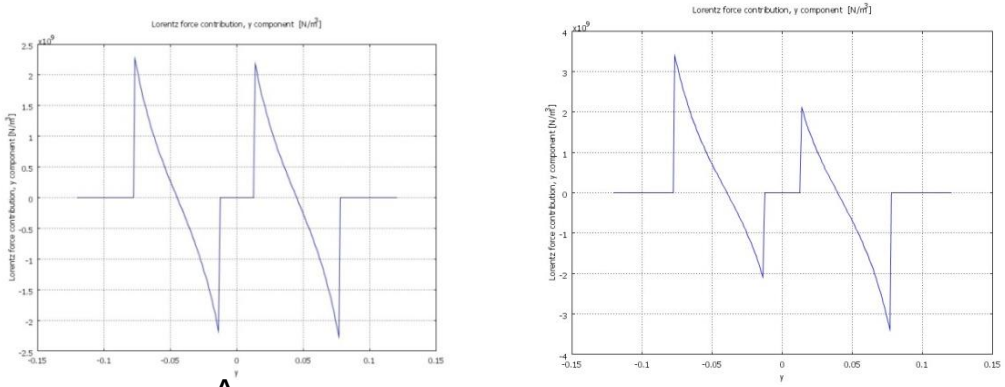

A B

Ampère forces (vertical component) acting on windings in vertical direction along a vertical line passing through a coil mid. A)- wiggler with iron yoke, B)- wiggler without iron yoke

The forces acting on windings, lead to their compression. Presence of iron yoke decrease integral force acting on windings.

3 groups of SC wiggler

High field SC multipole wigglers
(B=7-7.5 Tesla, λ~150-200 mm)

Medium field SC wigglers
(B=3.5-4.2 Tesla, λ~48-60 mm)

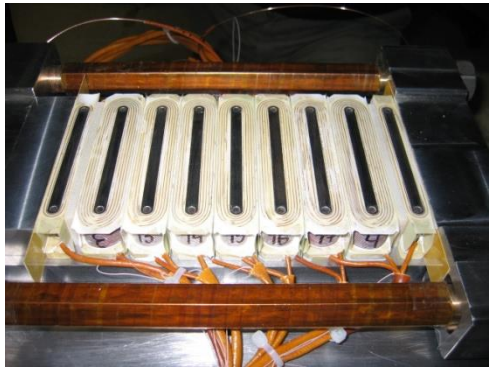

Short period SC wigglers
(B=2-2.2 Tesla, λ~30-34 mm

High field long period superconducting multipole wigglers are used for production of hard X-rays on storage rings with low electron energy (BESSY 1.7 GeV, CAMD LSU 1.35 GeV, Siberia-2 2.5 GeV, Dortmund university 1.5GeV)

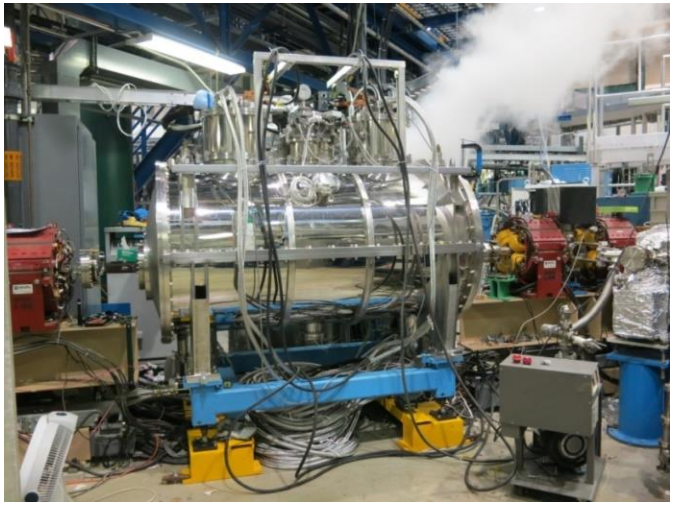

7.5 Tesla 15 pole superconducting wiggler (CAMD LSU, USA)

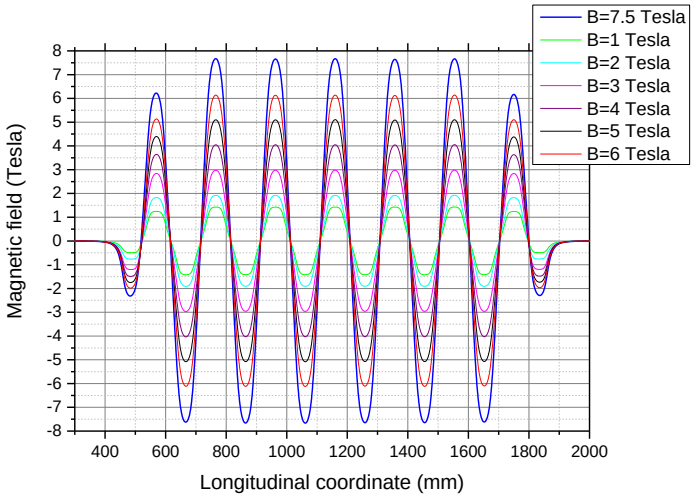

Magnetic field distribution at different field levels

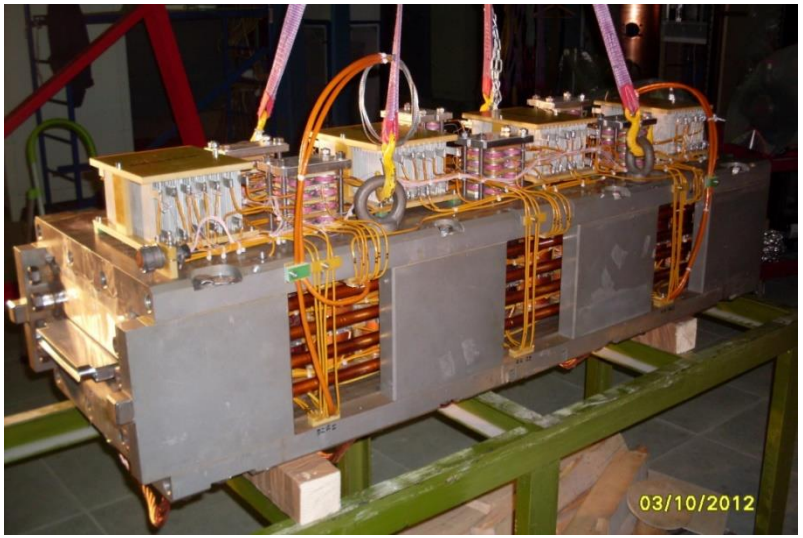

The installation of an insertion device with so high field at an accelerator working energy of 1.35 GeV is quite a complex accelerating challenge, as considerable effort was required for compensation of the influence of the magnetic field on the magnetic structure of the storage ring. All problems connected with the influence of the wiggler field on the beam dynamics were successfully solved during the wiggler commissioning with electron beam.

A PRELIMINARY REPORT FROM LOUISIANA STATE UNIVERSITY CAMD STORAGE RING OPERATING WITH AN 11 POLE 7.5 TESLA WIGGLER R. S. Amin et al, Proceedings of IPAC2015, Richmond, VA, USA

Training effect by quenching

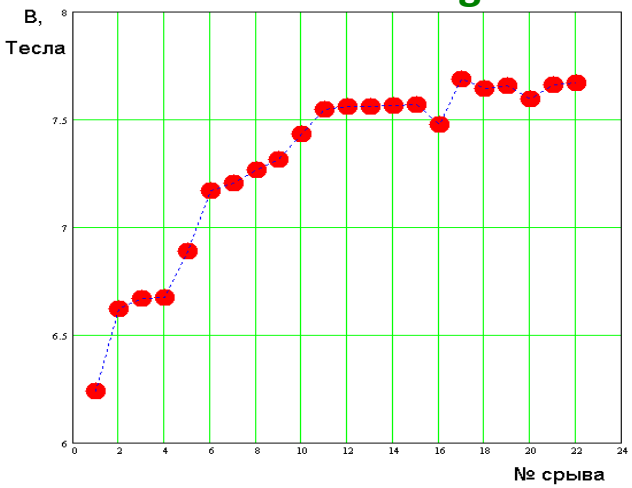

Quench history 7T superconducting wiggler for BESSY-HMI during test in bath cryostat

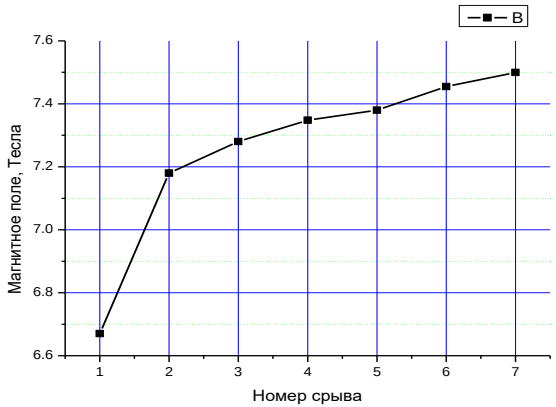

Quench history 7.5T superconducting wiggler for Siberia-2 during test in bath cryostat

Superconducting wire parameters for wigglers
With high stored energy

wire diameter,mm	0.85 (0.92 with insulation)
Ratio NbTi:Cu	1:1.4
Critical current, A	380 (at 7 Tesla)
filaments number in the wire	8910

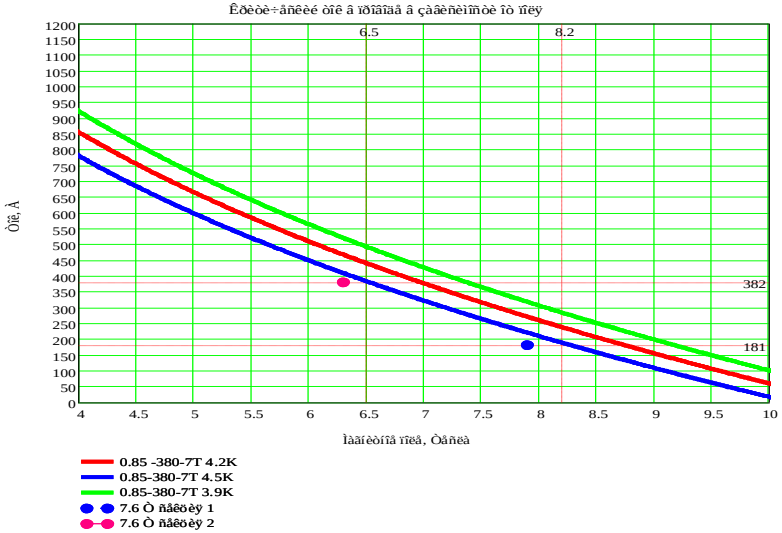

Critical curve of the SC wire at various temperatures. Points represent values of currents and the maximal fields on a winding in 1-st and 2-nd sections at the maximal field in median planes of 7.5 Tesla.

Superconducting multipole wigglers with medium period are used for production of hard X-rays on storage rings with electron energy ~3 GeV (Canadian Light Source, Diamond Light Source, Australian synchrotron, Brazilian Light Source, German Light Source ANKA) to increase a photon flux significantly (10-100 times)

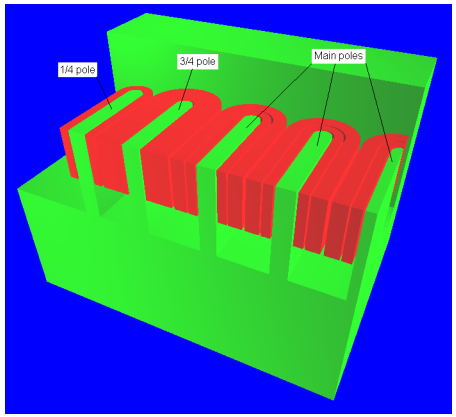

Model of the magnet for calculations

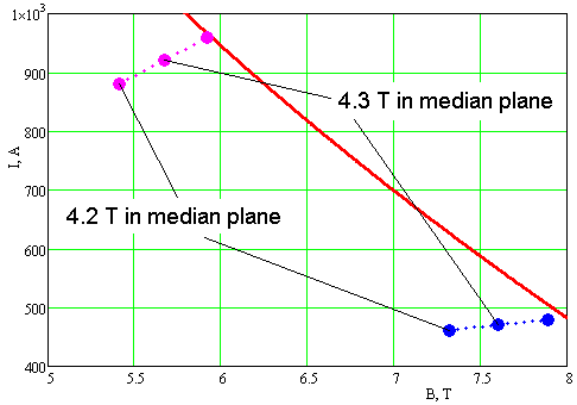

J-B diagram of the 2-sections coils of the wiggler

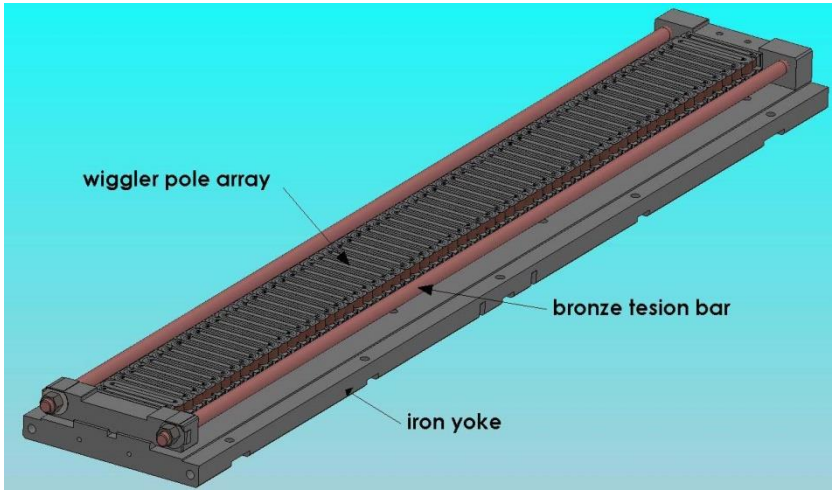

Drawing of the full length magnet (half)

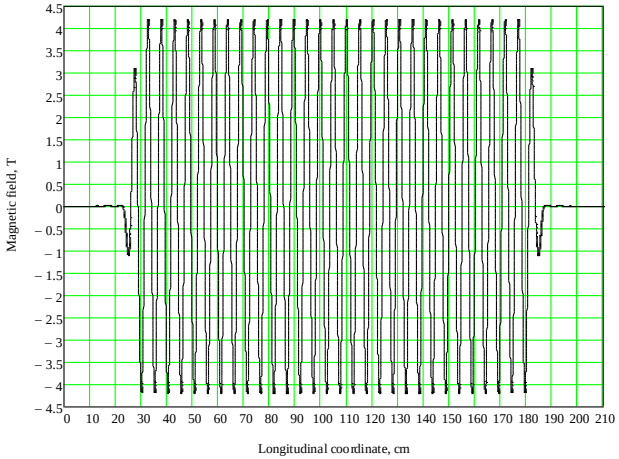

Magnetic field distribution in the wiggler

"Superconducting Multipole Wigglers: State of Art", Khrushchev S. et al, Proceedings IPAC 2014, Drezden, Germany

Superconducting multipole wigglers with medium period

- 2006 – 3.5 Tesla 49 pole for DLS, England
- 2007 – 4.2 Tesla 27 pole SCW for CLS, Canada
- 2009 – 4.2 Tesla 49 pole SCW for DLS, England
- 2009 – 4.1 Tesla 35 pole SCW for LNLS, Brasil
- 2012 – 4.2 Tesla 63 pole SCW for ASHO, Australia
- 2013 – 2.5 Tesla 40 pole SCW for ANKA CATACT beamline
- 2015 – 3 Tesla 72 pole SCW for ANKA-CLIC

DLS, England, 2006
49-pole 3.5 Tesla
superconducting wiggler
Period 60 mm

CLS, Canada, 2007
27- poles 4 Tesla
Superconducting wiggler
Period 48 mm

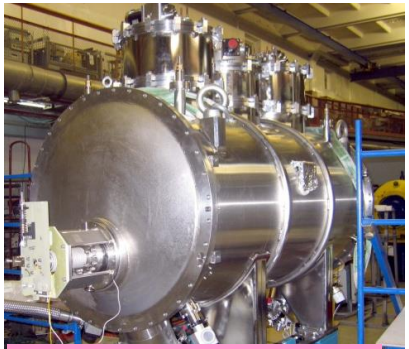

DLS, England, 2009
49-pole 4.2 Tesla
superconducting wiggler
Period 48 mm

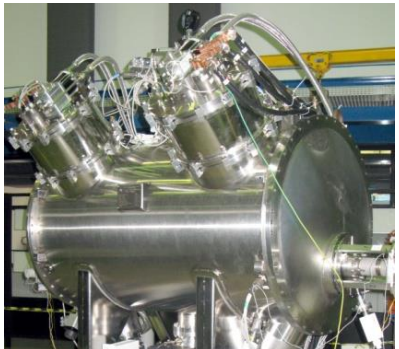

LNLS, Brazil, 2009
35-pole 4.2 Tesla
superconducting wiggler
Period 60 mm

AS, Australia, 2012
49-pole 3.5 Tesla
superconducting wiggler
Period 52 mm

ANKA, Germany, 2014
44- poles 2.5 Tesla
Superconducting wiggler
Period 48 mm

http://accelconf.web.cern.ch/AccelConf/r06/PAPERS/MONP03.PDF

http://accelconf.web.cern.ch/AccelConf/IPAC2014/papers/wepri091.pdf

"27-Pole 4.2 T wiggler for biomedical imaging and therapy beamline at the Canadian light source", NIM A603 (2009), p. 7-9.

ANKA, Germany, 2015
72- poles 2.9 Tesla
Superconducting wiggler
Period 51 mm

4.2 Tesla 49-pole superconducting wiggler
DLS (England)

I12 beamline - JEEP: Joint Engineering, Environmental and Processing

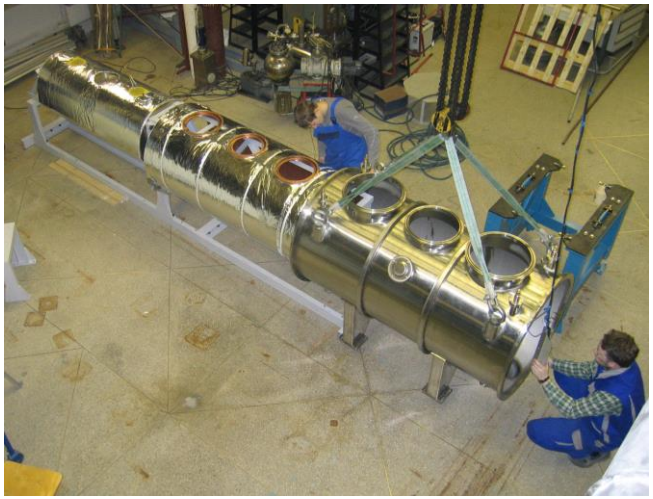

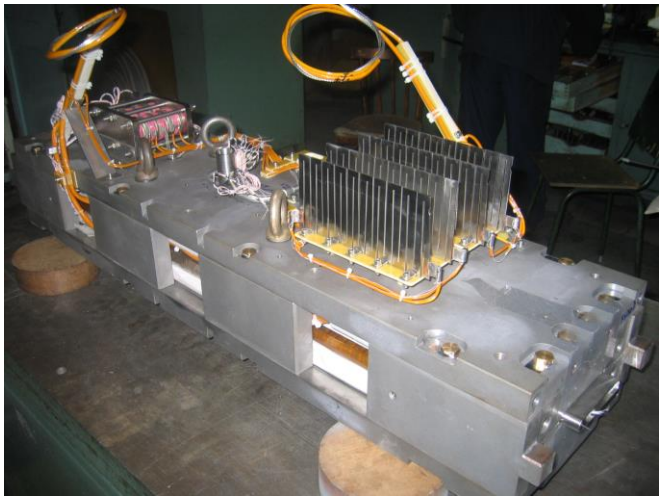

Main Research Techniques: (50-150 кэВ) Imaging and tomography, X-ray diffraction, Small Angle X-ray Scattering (SAXS), Single Crystal Diffraction, Powder diffraction

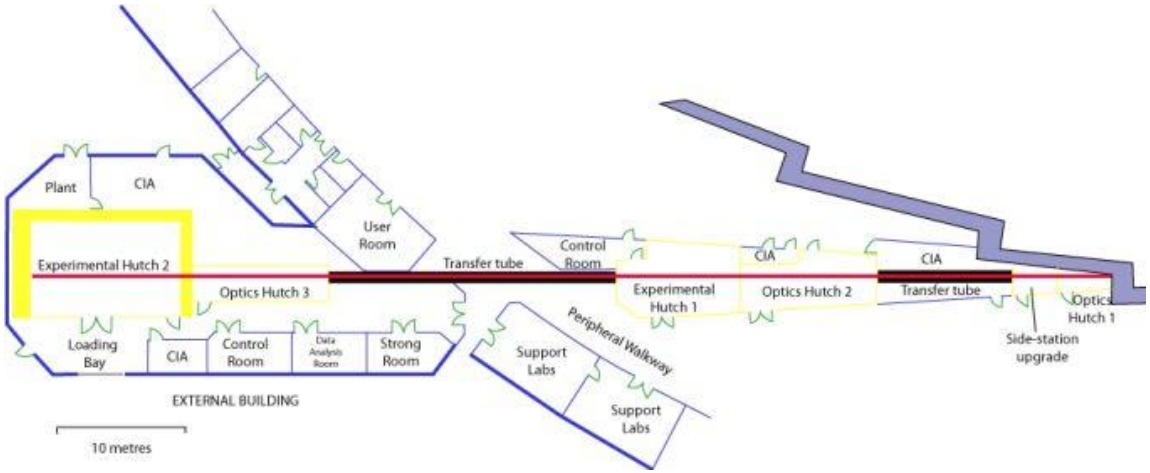

Superconducting multipole wigglers with medium period

Angular-spectral photon distribution from the wiggler (63 poles):
B_0=4.2T, E=3 GeV, I=0.2 A,

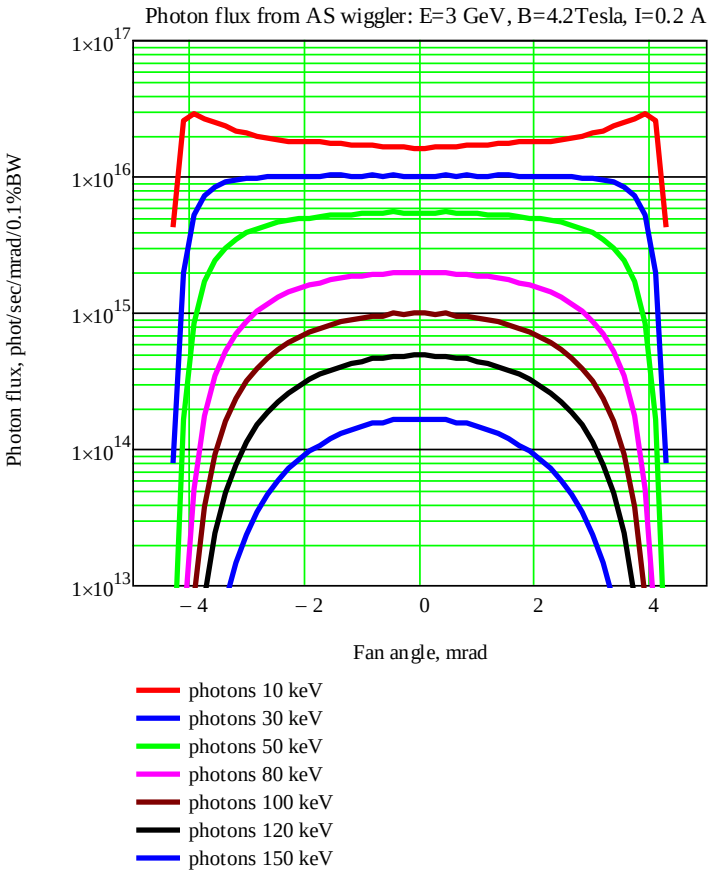

Australian Light Source

Assembled magnet

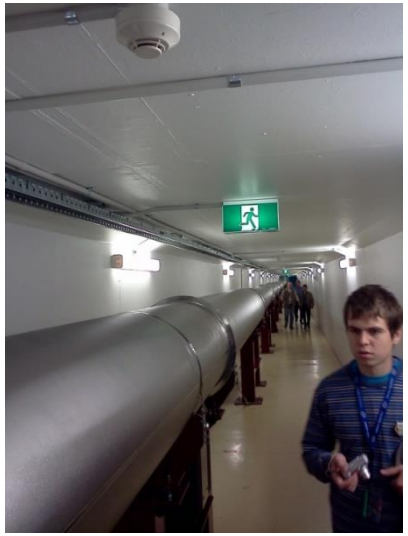

140 m long Imaging and medical beamline

End of beamline- extraction window

Quench training effect of MP superconducting wigglers

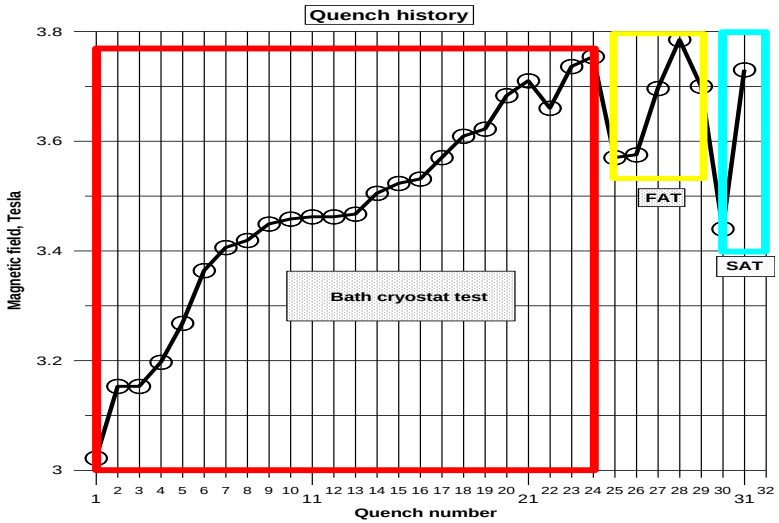

Quench history of 3.5T superconducting wiggler for DLS during test in bath cryostat, FAT and SAT

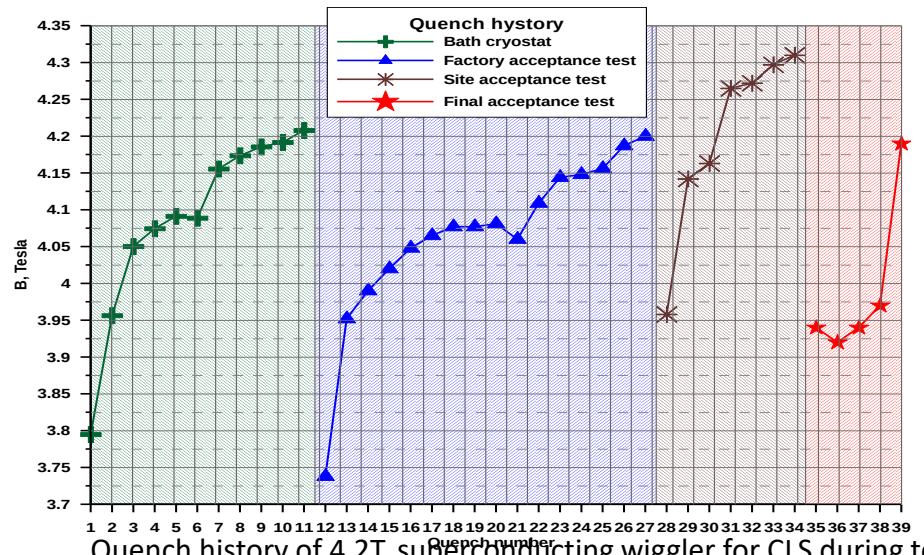

Quench history of 4.2T superconducting wiggler for CLS during test in bath cryostat, FAT and SAT

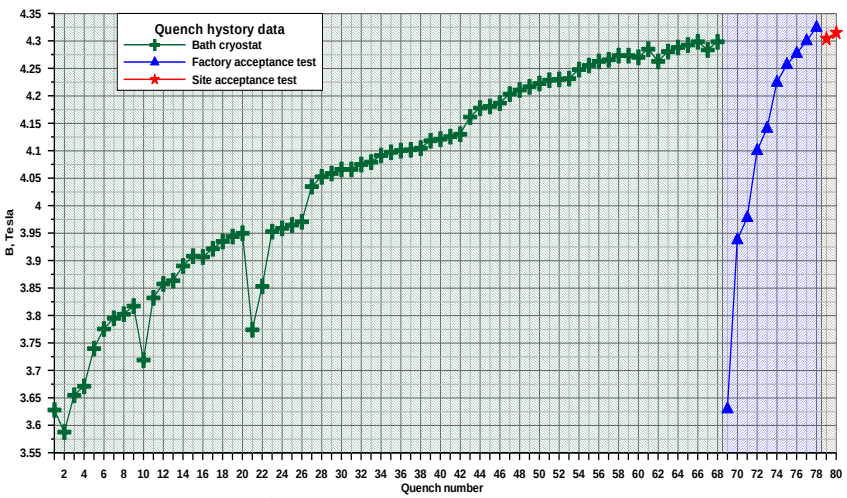

Quench history of 4.2T superconducting wiggler for DLS during test in bath cryostat, FAT and SAT

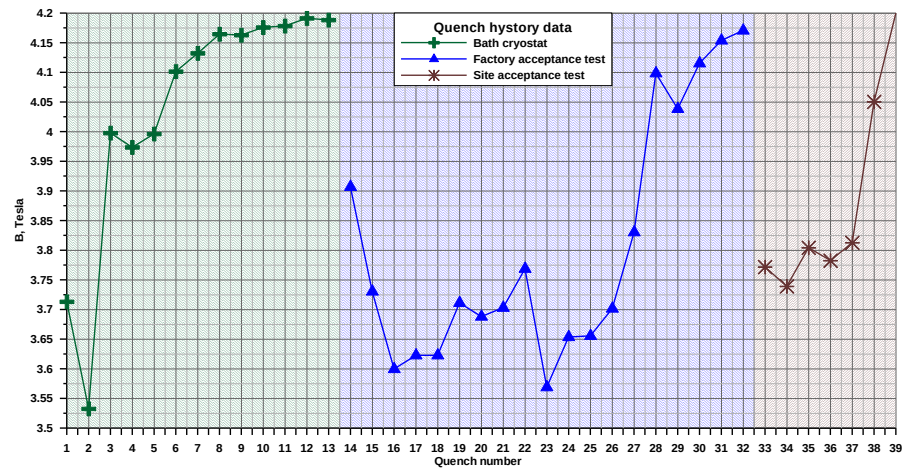

Quench history of 4.2T superconducting wiggler for LNLS during test in bath cryostat, FAT and SAT

Short period superconducting multipole wigglers

Longitudinal magnetic field distribution

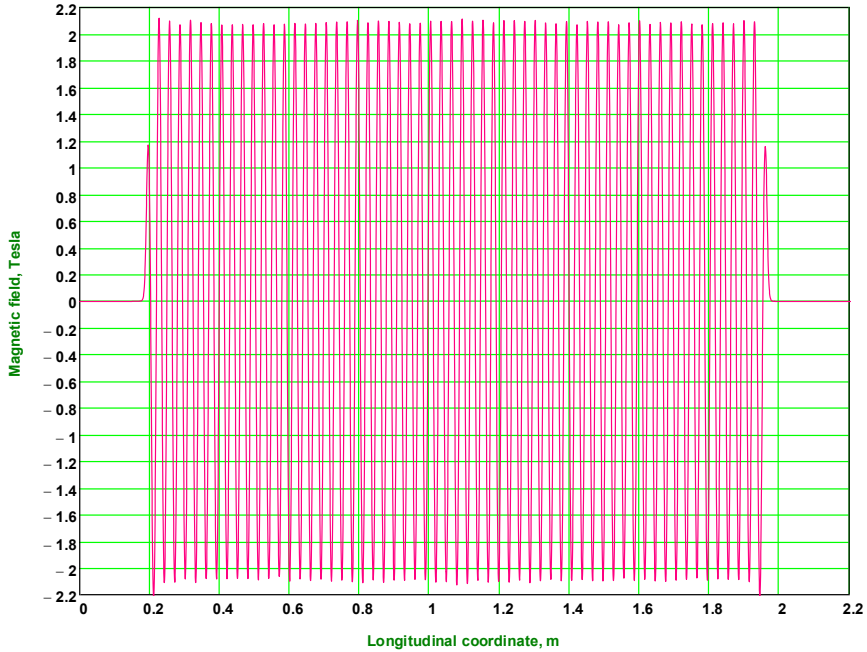

119-pole 2.1 Tesla SC wiggler for ALBA CELLS

½ of the wiggler magnet

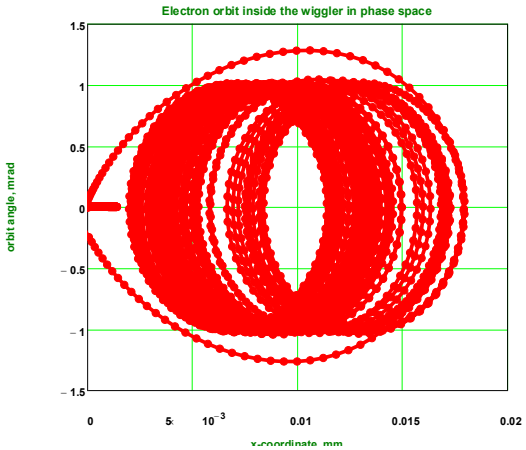

Electron beam orbit in x-x` coordinate

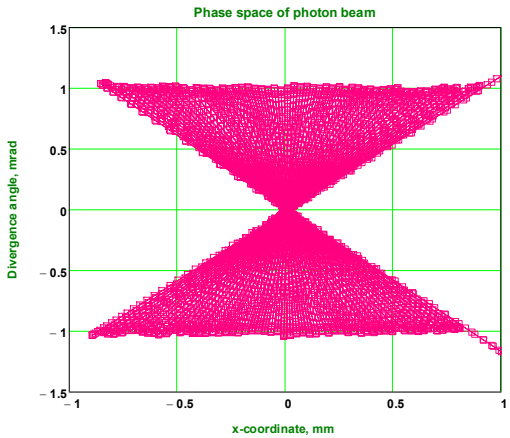

Phase space of the photon beam

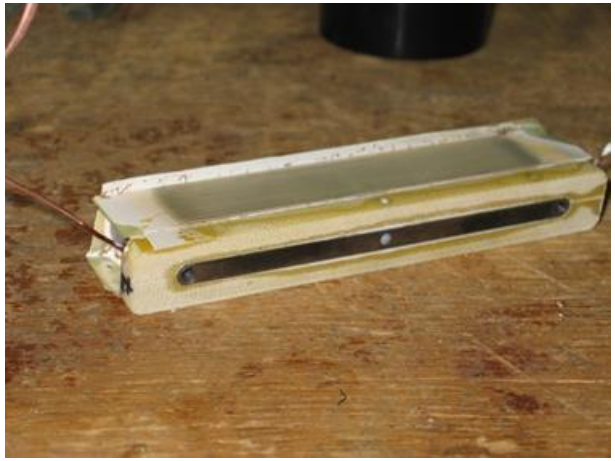

Magnet pole – main element of the magnet

Short period superconducting multipole wigglers

119-pole 2.1 Tesla SC wiggler for ALBA CELLS

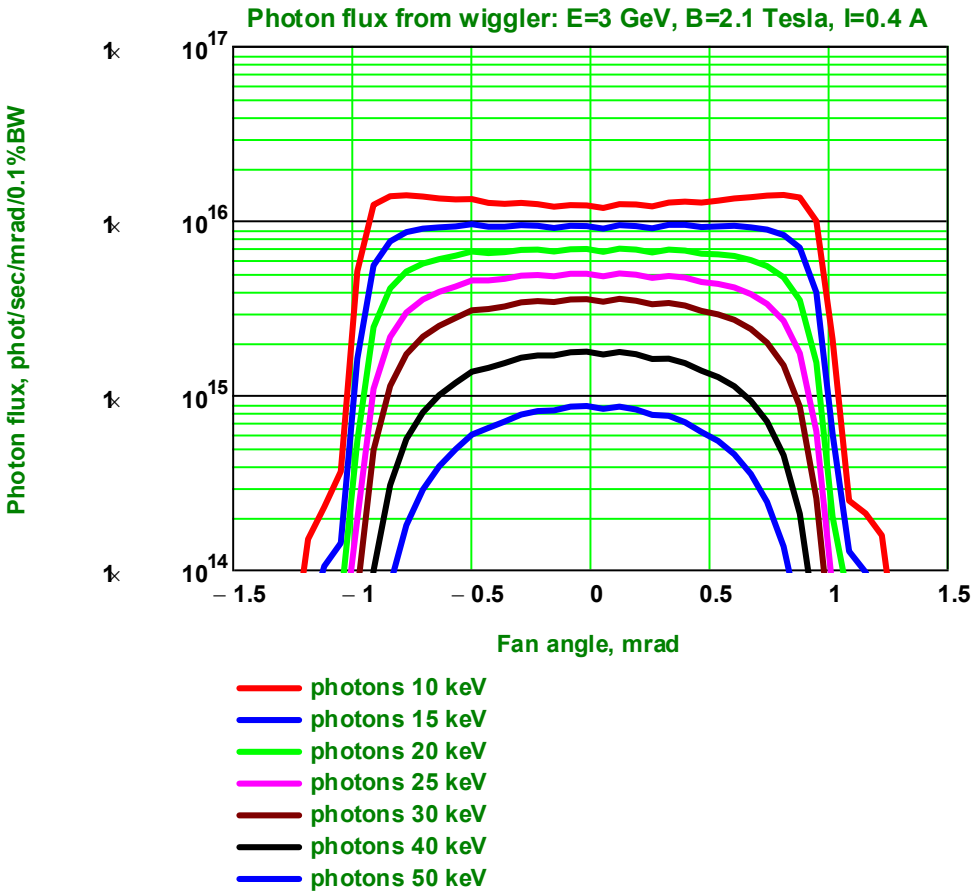

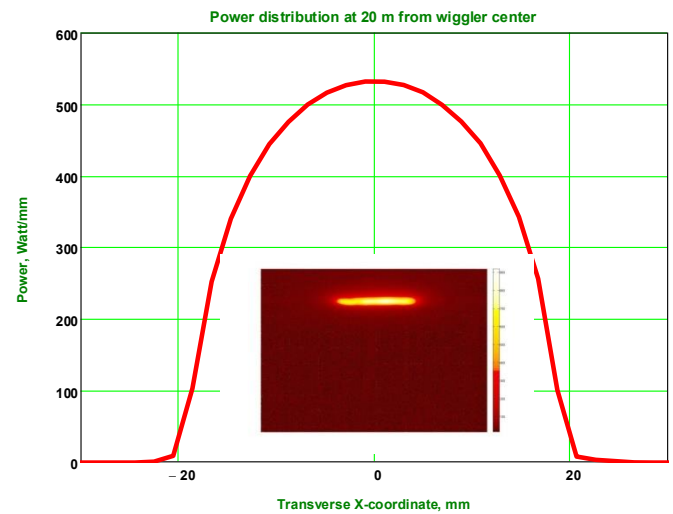

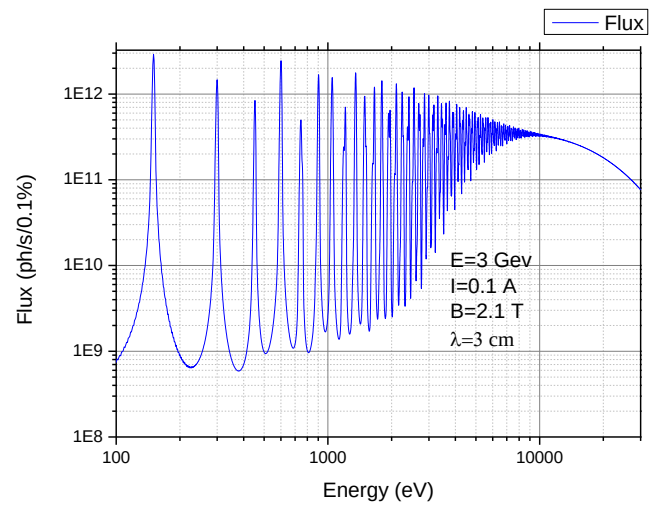

Spectrum photon flux through 1x1 mm^2 at 30m

"Superconducting 119-pole wiggler with a 2.1 T field and 30-mm period length for the ALBA storage ring", Volkov A. et al, Journal of Surface Investigation 6 (3) p. 379-387

Horizontal racetrack type (SC wigglers)

Budker Institute of Nuclear Physics

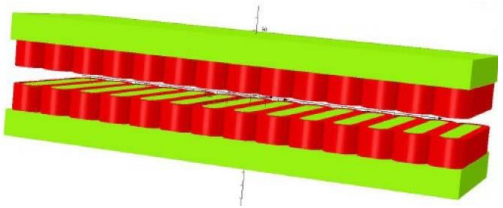

Magnet array of horizontal racetrack type poles (example of 30 mm period SC 2.1T wiggler)

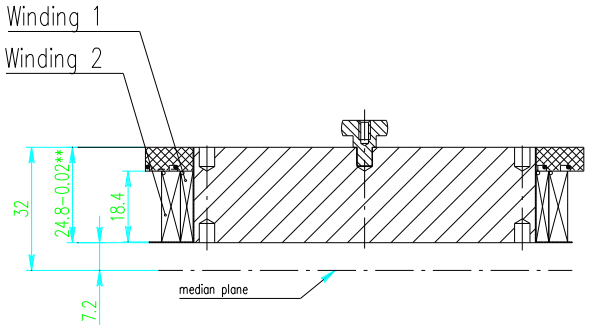

Drawing and photo of racetrack type poles (example of 2-sections coil of 48 mm period 4.2T wiggler

Horizontal racetrack coils assembly allows :

•to pre-stress all coils together for compensation of magnetic pressure

•to use 2 or more sections coils, which gives a possibility to obtain higher field for the same SC wire.

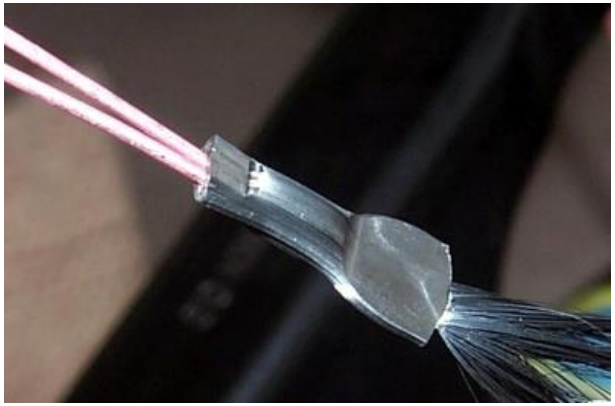

Cold welding method of wires connection gives resistance of the connection10^{-10}-10^{-13} Ohm

Superconducting shifters

Superconducting Wave Length Shifters

Standard Wave Length Shifter (WLS) consists of 3 bending magnets. The central dipole is used as a source of radiation, two other side dipoles are used as correcting magnets for a beam orbit compensation of an action of the central magnet on beam orbit.

The main requirement of distribution of a magnetic field is an equality of the zero 1st and 2nd integrals of a field:

$$I_1 = \int_{-L/2}^{L/2} B_z(s)ds \qquad I_2 = \int_{-L/2}^{L/2} ds' \int_{-L/2}^{s'} \frac{B_z(s'')}{B\rho} ds''$$

An example of 10Tesla shifter for Spring-8

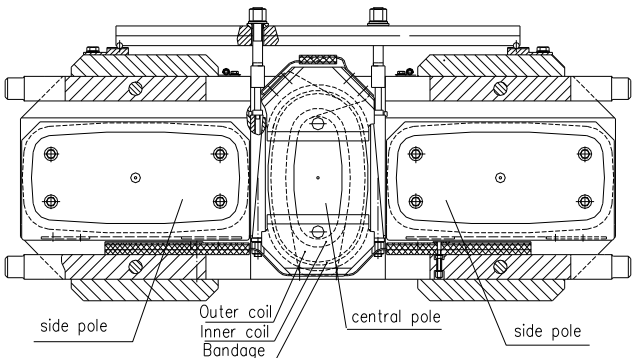

Cross section in median plane of 10 Tesla WLS

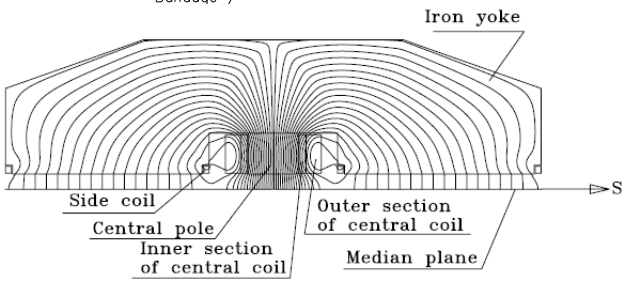

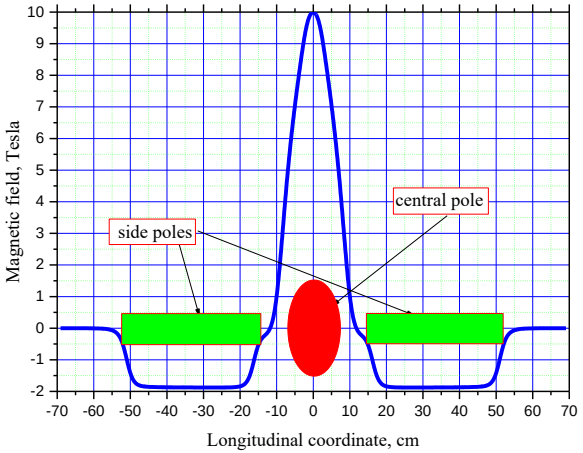

Longitudinal magnetic field distribution

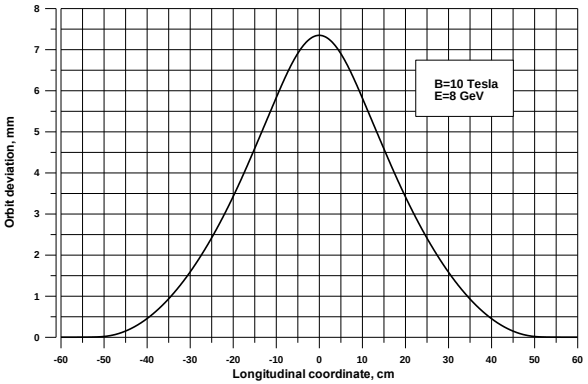

Orbit distortion inside the WLS

Journal of Synchrotron Radiation (1998), Vol.5, Part 3, p.360-362. Ando A. et al

10Tesla superconducting WLS

Pole number	3
Magnetic field in central pole (median plane)	10 Tesla (10.3 Tesla maximum)
Magnetic field in side poles (median plane)	1.9 Tesla
Stored energy at 10 Tesla field	~400 kJ
Weight of wiggler cold part	~1000 kG
Windings of the central pole	
Nb_3S – Rectangular wire by the size	0.85x1.2 мм^2
Nb-Ti – Round wire by a diameter	0.92 мм
Full length of the magnet	1000 mm
Pole gap	42 mm
The size of the electron vacuum chamber	100x20 mm^2

Nuclear Instruments and Methods in Physics Research. –2000. – V.A448, Nos.1, 2. – P.51-58.

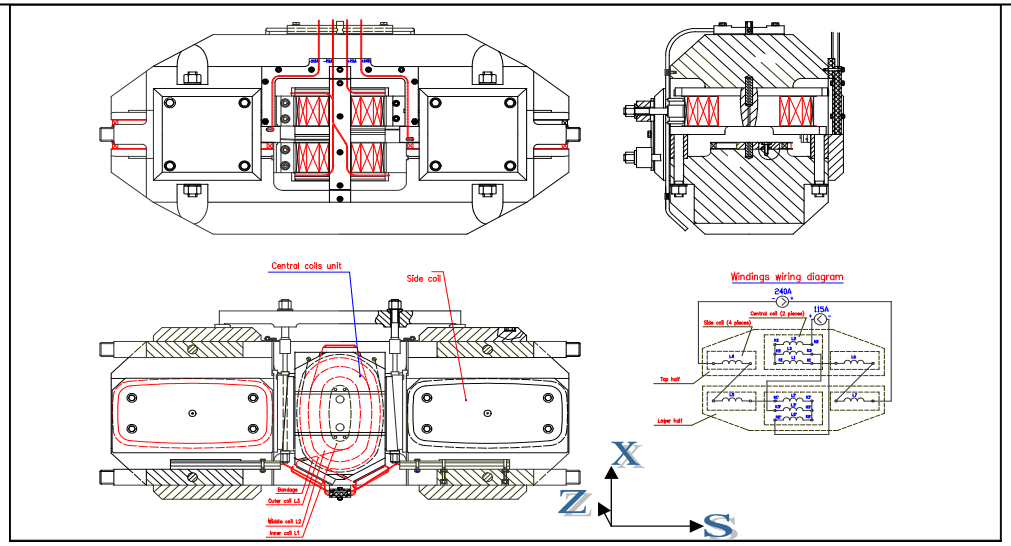

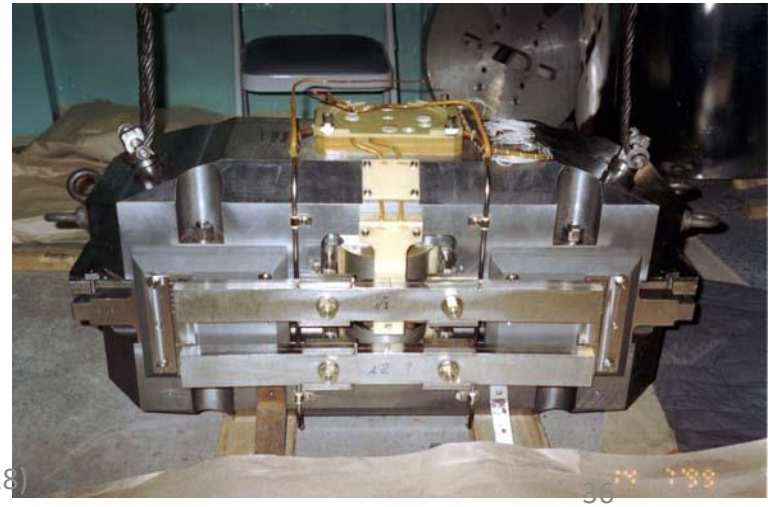

Superconducting Wave Length Shifters

Wave Length Shifter with fixed point of radiation – consists of 5 bending magnets. The central pole is used as photon source. Other poles are used for electron orbit alignment outside the shifter and to keep zero displacement of the electron orbit at the radiation point of the central pole.

Example of SC 7 Tesla shifter for BESSY as primary radiometric source standard in the X-ray range.

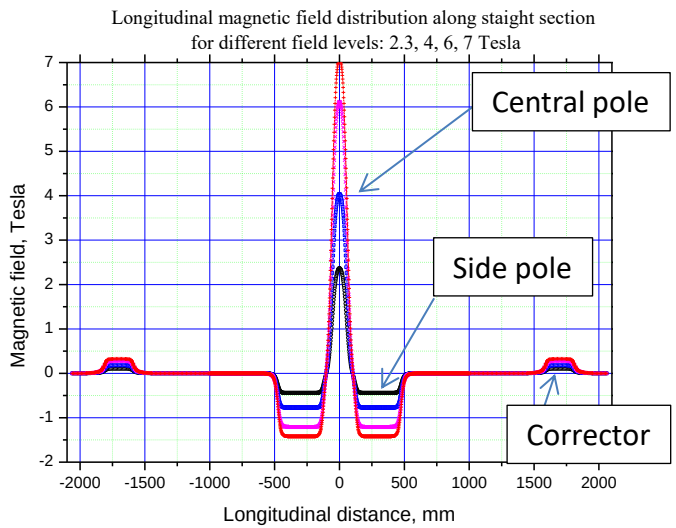

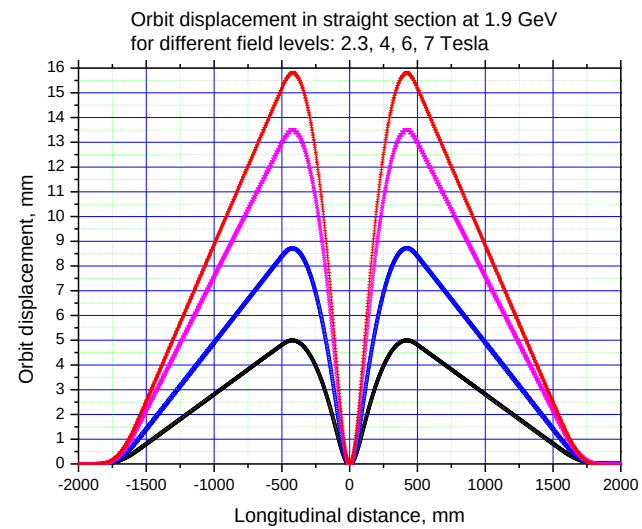

The spectrum of radiation from the central magnet of the WLS is precisely known due to calculations which require electrons energy, current of electrons and a magnetic field in the radiation point.
The magnetic field in the center of the magnet may be changeable within 2-7 Tesla and the field value is measured with high precision by means of a Hall sensor calibrated by means of a nuclear magnetic resonance sensor.

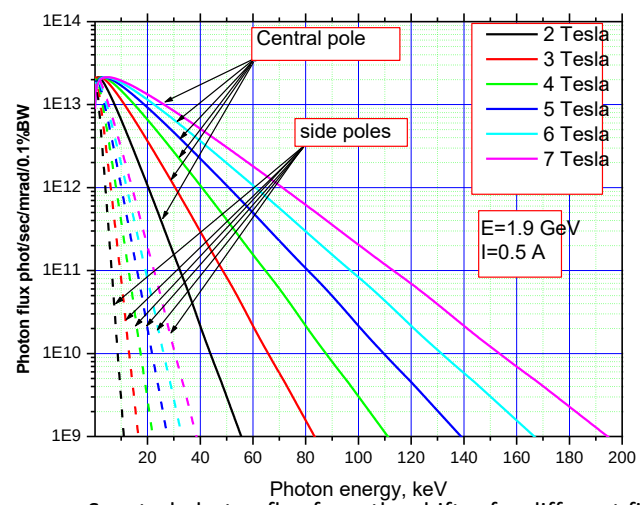

Spectral photon flux from the shifter for different field

Nuclear Instruments and Methods in Physics Research A 467–468 (2001) 181–184
Nuclear Instruments and Methods in Physics Research Section A: Accelerators, Spectrometers, Detectors and Associated Equipment Volume 580, Issue 3,, Pages 1536–1543

Superconducting undulators

Superconducting undulators

Magnetic structure layout

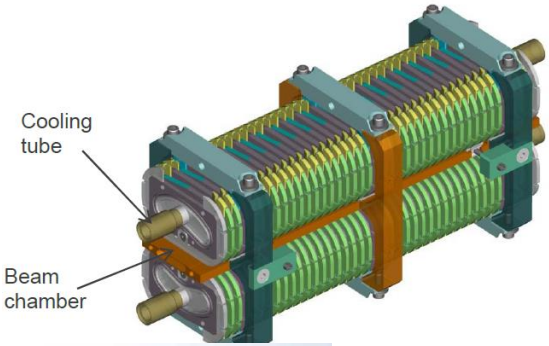

Argonne NATIONAL LABORATORY

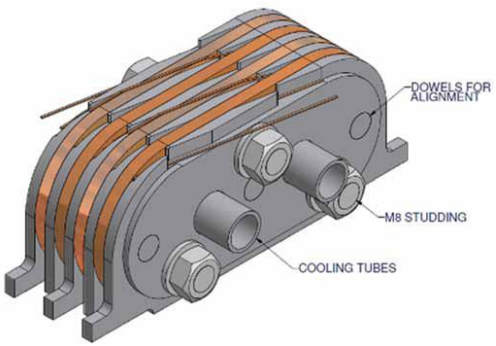

ASTeC

Vertical racetrack coils

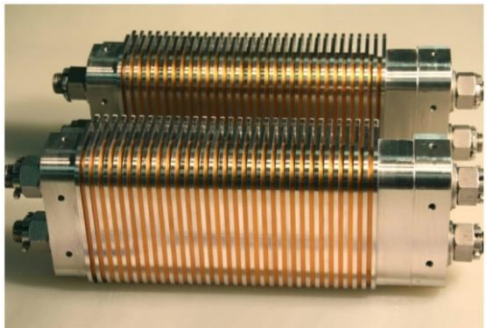

BABCOCK NOELL

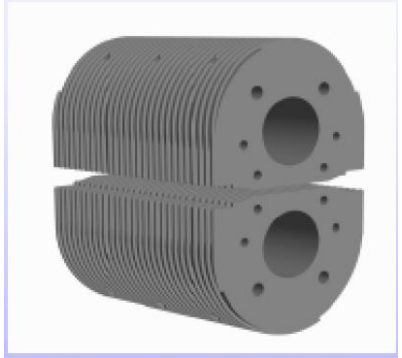

Prototype undulator (Mock-up)

ACCEL

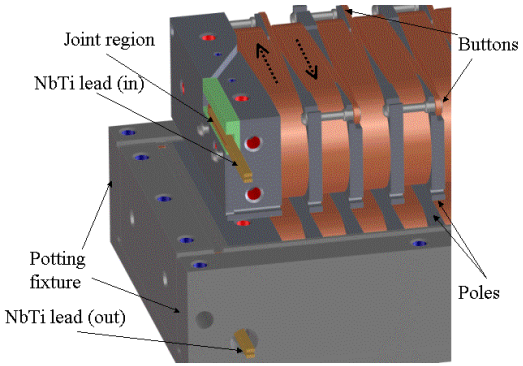

LBNL

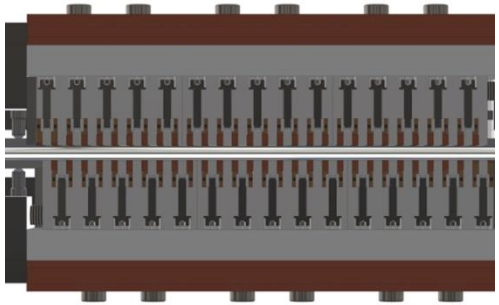

Budker INP, horizontal racetrack

Undulator radiation spectrum

Period λ=15.6mm, L=2 m, Energy 3 GeV, I=0.1 A

$$K = 0.934 \cdot \lambda_0[\mathrm{cm}] B_0[\mathrm{T}]$$

K=0.5

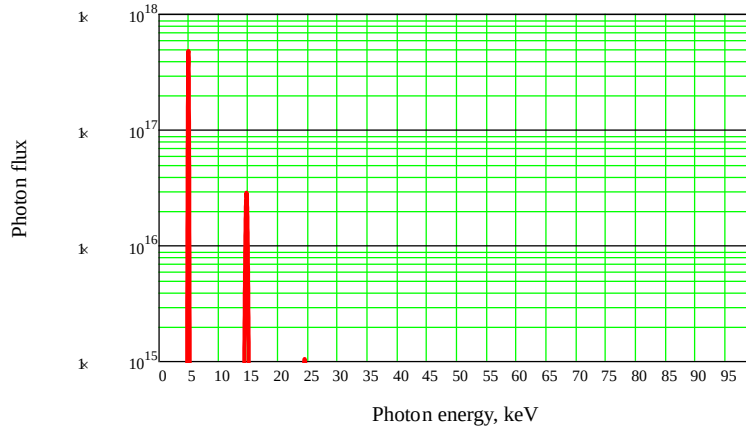

K=1

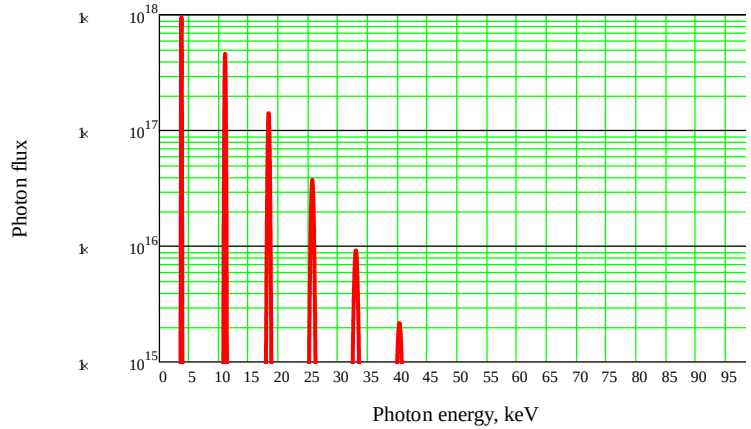

K=2

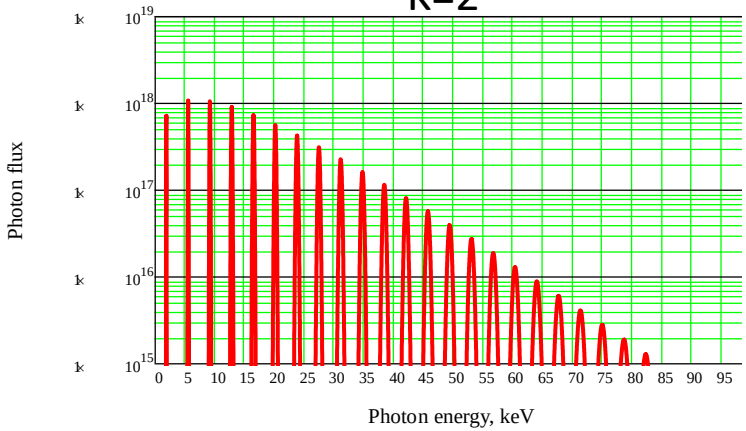

K=4

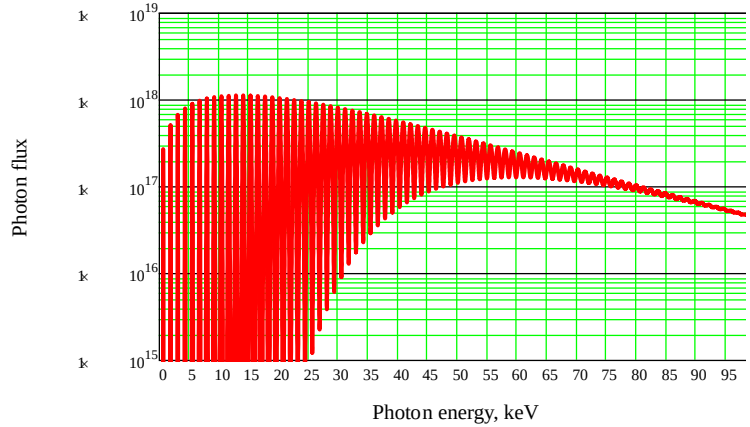

Superconducting undulators

The fundamental difference between undulator and wiggler consists in the emission spectrum, which unlike wiggler, undulator spectrum is discrete spectrum:

$$\varepsilon_n = 0.95n \frac{E^2[GeV]}{\left(1+\frac{K^2}{2}\right)\lambda_u[cm]}$$

K= $0.934B[T]\lambda_u$[cm]

n-harmonic number
E-beam energy
B-field amplitude
λu-undulator period

To obtain a constructive superposition of radiation from different poles of the undulator, it is necessary to reduce the phase error in the radiation fields:

Phase error calculation

$$x'(z) = \frac{e}{\gamma mc}\int_0^z B\, dz \qquad \varphi(z) = \frac{2\pi}{\lambda_0}\left(\frac{z}{2\gamma^2} + \frac{1}{2}\int_0^z x'^2\, dz\right)$$

Large phase error leads to an exponential decrease in the radiation intensity in the spectrum line:

$$I_n \sim e^{-(n\varphi)^2}$$

To obtain a phase error of less than 3˚ the manufacturing errors of the magnet elements must be within 10 microns.

Cryogenic systems of superconducting insertion devices

Cryogenic system

BATH CRYOSTAT WITH CRYOCOOLERS

The primary goal of the cryostat design is to create reliable safe systems with the possibility of long term independent work with close to zero liquid helium consumption. Cryocoolers are used for cooling the shield screens and heat coming from normal conducting current leads due to their heat conductivity and Joule heat.

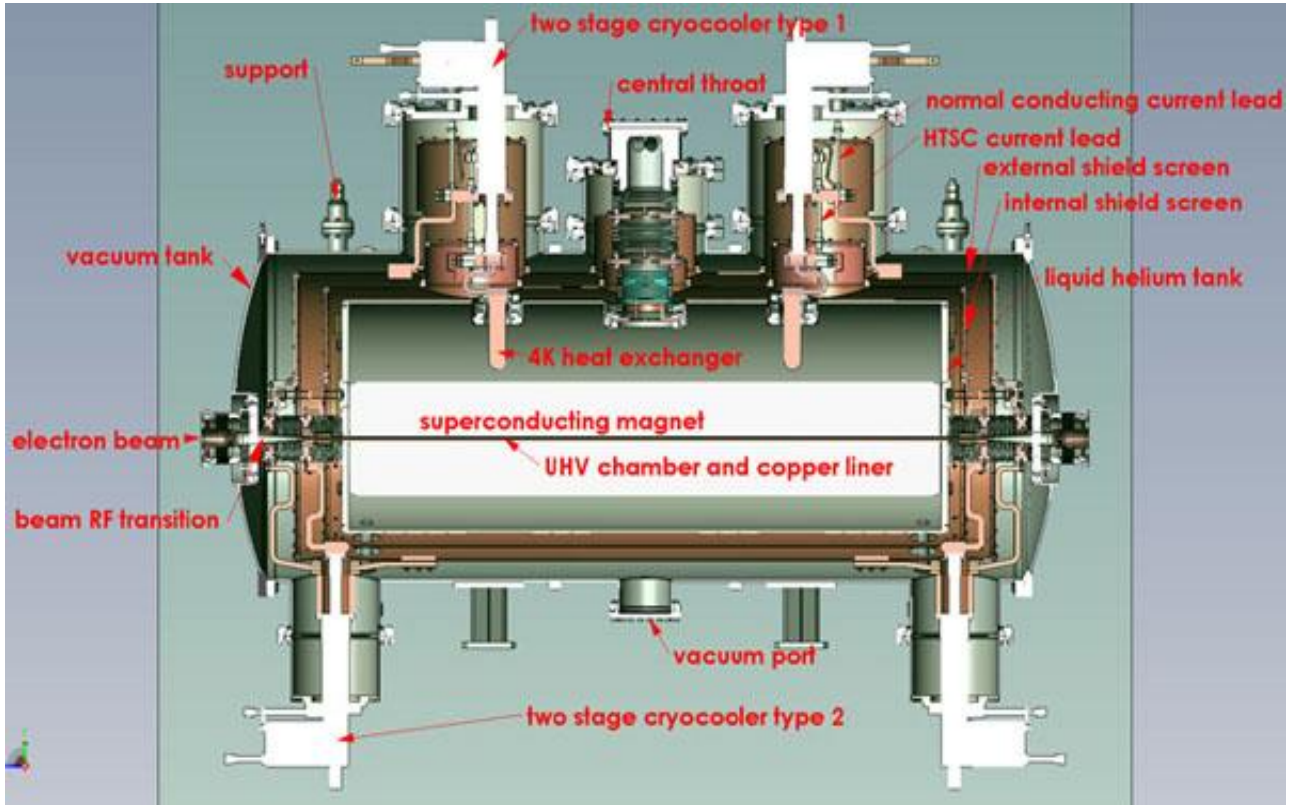

Horizontal bath cryostat for a wiggler magnet

In order to provide zero liquid He consumption four 2-stage cryocoolers are used symmetrically situated relatively of the wiggler ends. The basic cryostat is to prevent of any heat to penetrate into the liquid He tank intercepting it by heat sinks connected to the cryocoolers stages. Two cryocoolers with stages of 4K and 50K (type 1) and two cryocoolers with stages of 10K and 50K (type 2) are used for this aim.

Cryogenic system

Beam vacuum chamber and copper liner for medium field wiggler

The second stages of the cryocoolers with 20K stage are used for cooling down of 20K shield screen and for interception of released heat in the copper liner when the electron beam is passing through the liner.

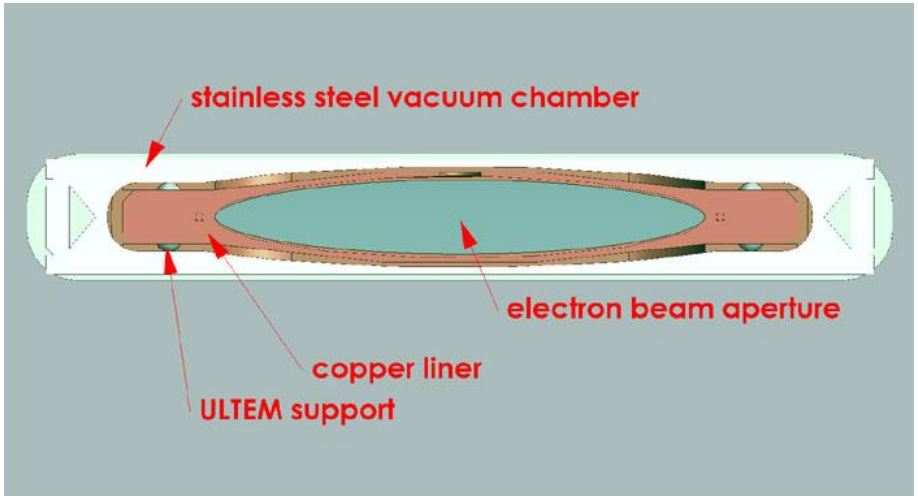

Cross section of cold vacuum chamber with copper liner inside for wiggler with medium magnetic field

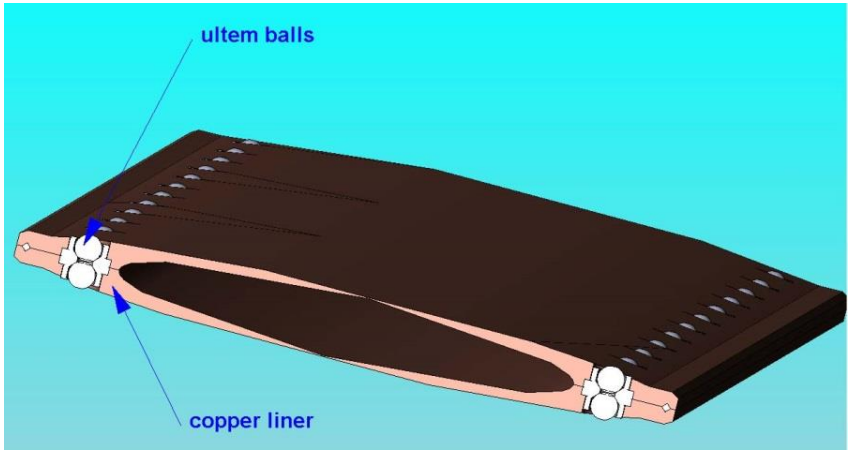

Copper liner with ULTEM support

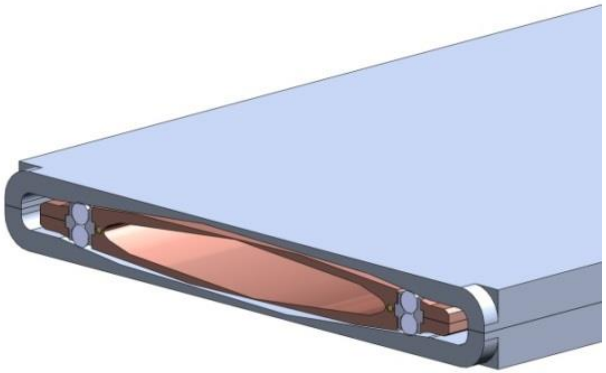

Copper liner assembled with vacuum chamber

Vacuum chamber and copper liner

Insulating vacuum is separated from UH vacuum of a storage ring and keep at vacuum level 10^{-6} – 10^{-7}Torr by 300l/s ion pump

Beam vacuum chamber system

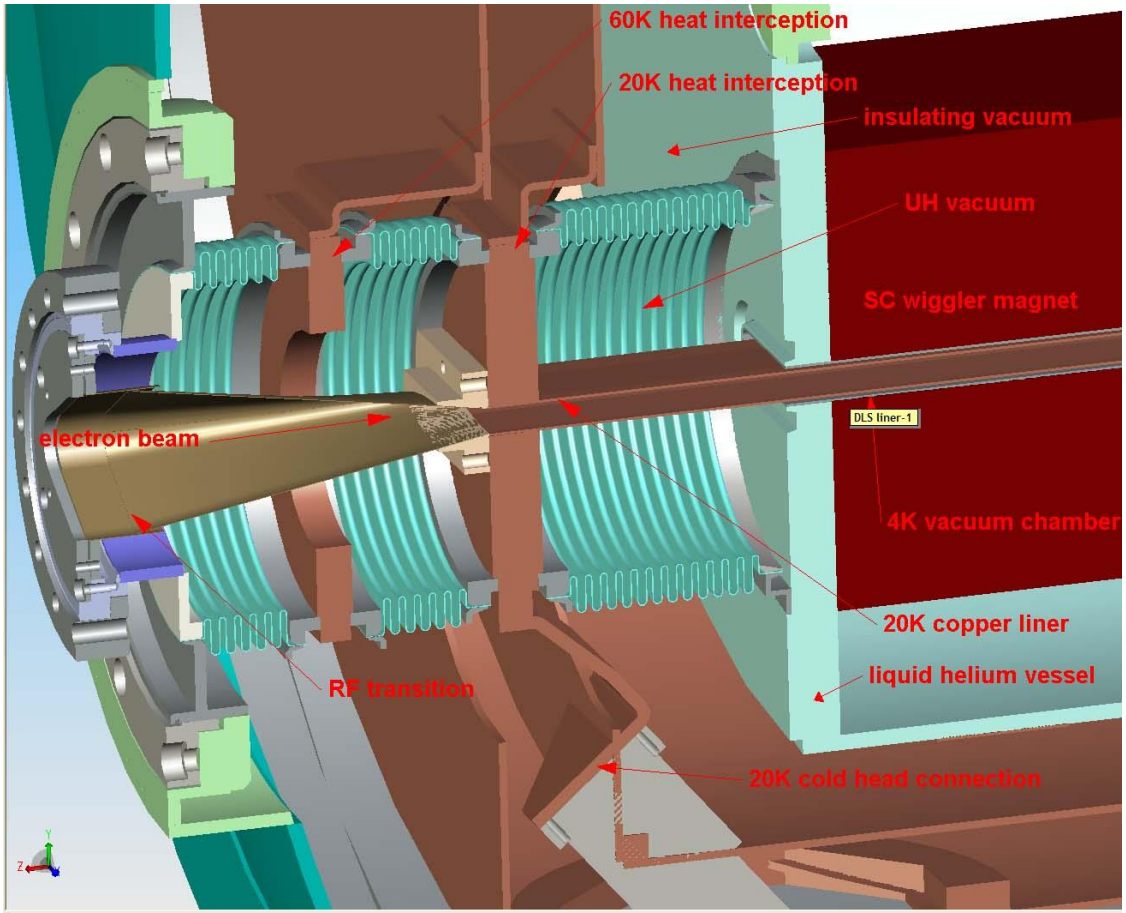

Liquid helium vessel with vacuum chamber fittings

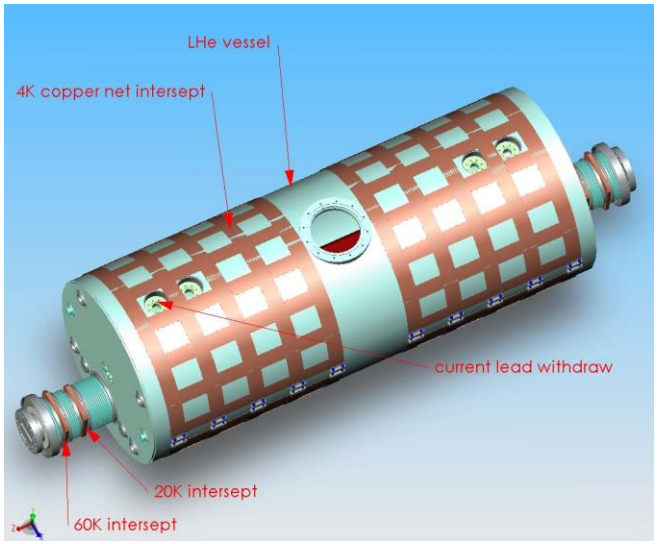

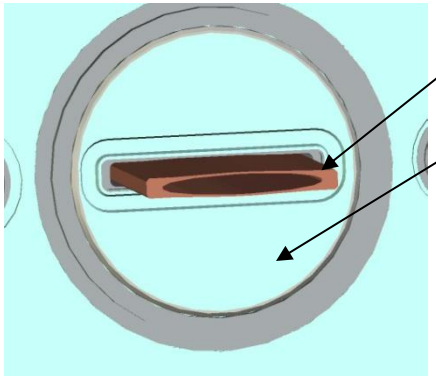

Cryogenic system

Cryostat with indirect cooling system

The wiggler cooling system is based on indirect cooling of the superconducting wiggler by LHe boiling in two copper tubes. In the current design, there are ***two*** cooling tubes attached to the copper plate of the upper half of the wiggler. The lower half is cooled via copper links of high thermal conductivity. Liquid helium is stored in the LHe vessel positioned above the wiggler.

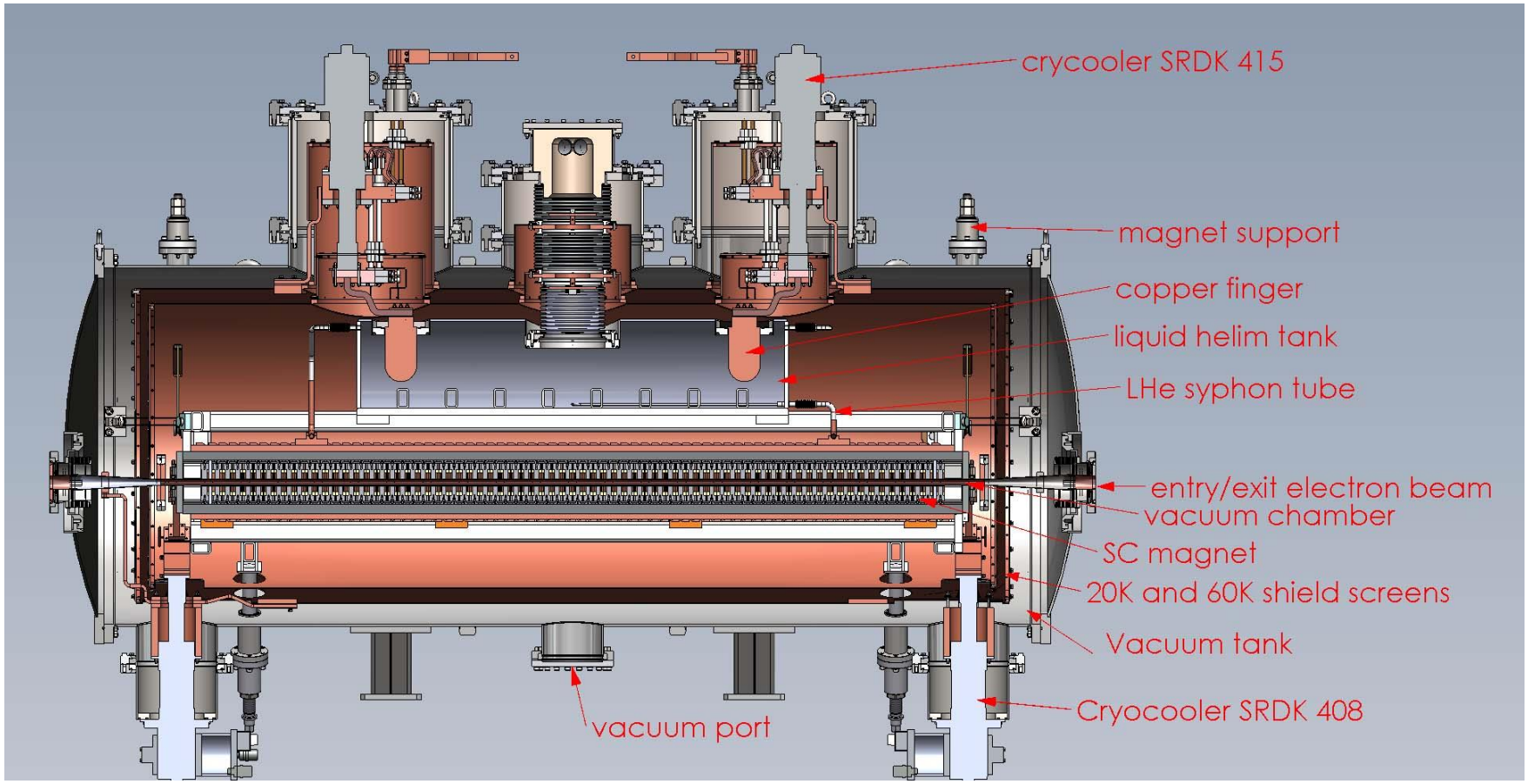

Cryogenic system

Cryogenic system of SC insertion devices progress (Budker INP)

1979

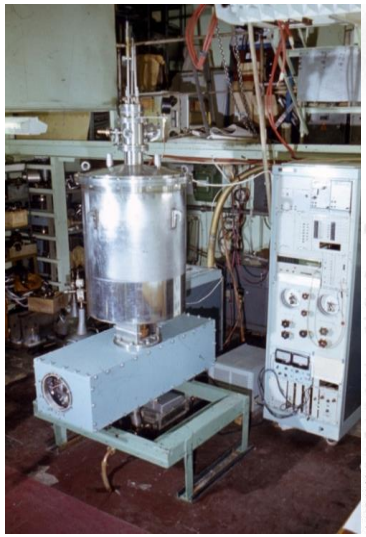

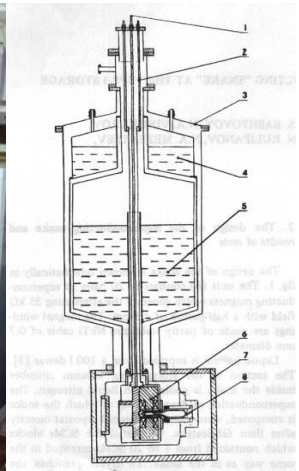

Fig. 1. A general view of the snake for the storage ring VEPP-3; 1 – liquid helium supply pipe, 2 – current leads, 3 – dewar, 4 – liquid nitrogen, 5 – liquid helium, 6 – superconducting magnets, 7 – vacuum container, 8 – storage ring vacuum chamber.

Liquid helium consumption ~ **4 l/hr**

2002

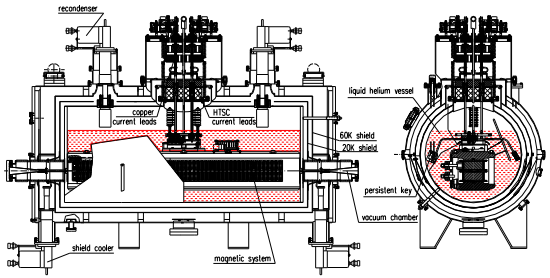

Liquid helium consumption ~ **0.6 l/hr**

2015

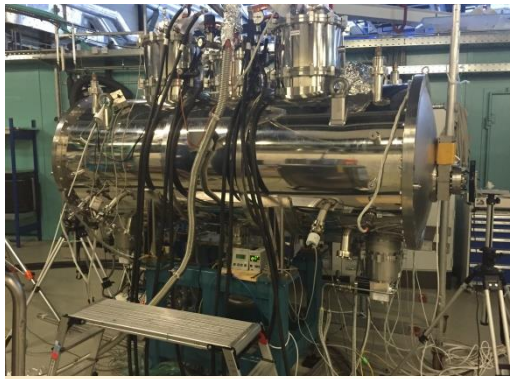

Indirect cooling system. Liquid helium used as cooling agent

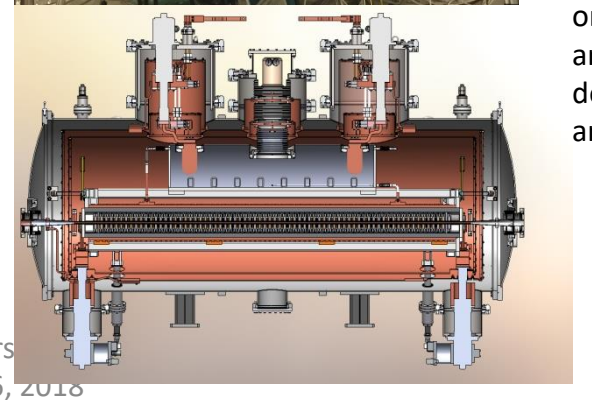

For initial cooling of the magnet thermal tubes on the basis of nitrogen and helium are developed, fabricated and tested.

2007

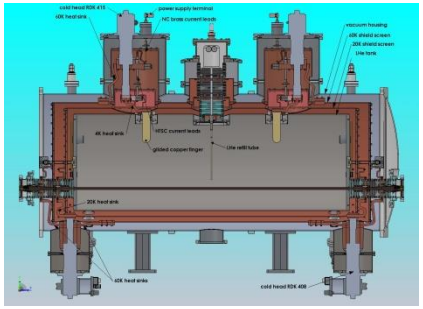

Liquid helium consumption < **0.03 l/hr**

Cryogenic system

*SCU cryogenic system (*Advanced Photon Source (APS) at Argonne National Laboratory)

The first APS SCU cryogenic system was a standalone cryostat with four Sumitomo cryocoolers

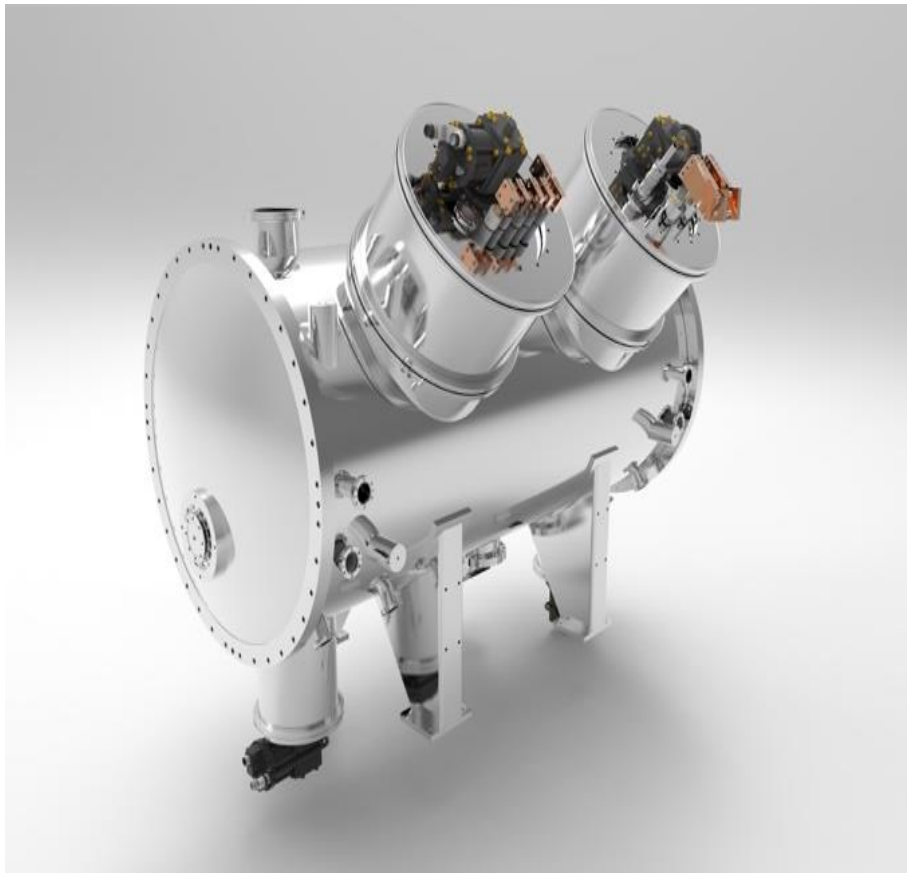

Rendering images (based on engineering drawings) of the APS original cryostat with four cryocoolers and internal second thermoshield .

Cryogenic system

Further modernization of the cryogenic SCU system at APS

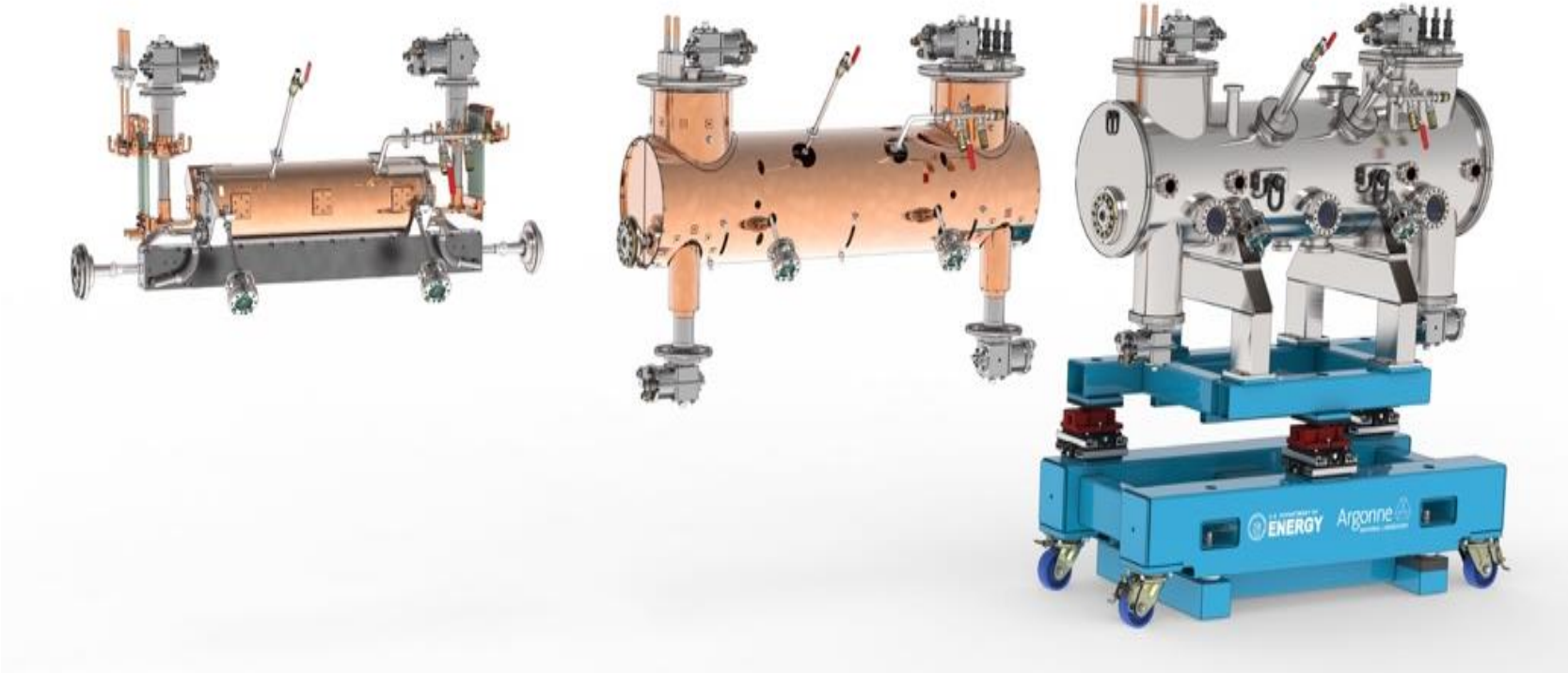

Rendering images (based on the engineering drawings) of new APS SCU cryostat with thermal shield, cold mass, undulator and vacuum chamber.

Cryogenic system

The main parameters of the cryogenic systems low temperature superconducting insertion devices using cryocoolers :

- Allows continuous operation of the device for a long time (~1 year) in conditions of limited access to the system.
- In the normal operating mode (no power failures, unexpected quenches etc.) allows you to work with zero liquid helium consumption.
- Allows to decrease the temperature of magnets to ~3K, which gives an additional margin for the critical currents of the superconductor.
- Cooling time from room temperature to temperature of liquid helium and heating time is ~2-3 days.
- The cryostats using cryocoolers demonstrated high reliability for many years.

Thanks for attention